Supplement of Atmos. Chem. Phys., 16, 7213–7237, 2016
http://www.atmos-chem-phys.net/16/7213/2016/
doi:10.5194/acp-16-7213-2016-supplement

Atmospheric Chemistry and Physics
Open Access

Supplement of

Aerosol water parameterisation: a single parameter framework

Swen Metzger et al.

Correspondence to: Swen Metzger (s.metzger@cyi.ac.cy)

S1 Examples – Semi-volatile compounds

The following three sub-sections provide detailed examples for semi-volatile compounds, described in Sec. 2.4 (main text). The analytical solution is part of our new single parameter gas-liquid-solid partitioning framework and applied in Sec. 3 to mixed aerosol salt solutions through EQSAM4clim (see Appendix B and Sec. S2).

S1.1 Pure NH_4NO_3–gas-solid equilibrium (RH < RHD)

Gas-solid equilibrium of pure ammonium nitrate; NH_4NO_3 (index $_{AN}$) with $RH = 50$ % and below the RHD_{AN}= 61.83 [%] (Table 1), as illustrated in Fig. 3. The partial pressure product of gaseous ammonia, NH_3(g), and nitric acid, HNO_3(g) must equal or exceed K_p(T) to allow the formation of solid ammonium nitrate, NH_4NO_3(s). This is described by (R1) and the system can be solved with Eqs. (6–12). Note that in this case, only the gas phase concentrations are required to solve (R1), since the concentrations of solids are treated as unity. Here, all concentrations denoted by [ ] are given in $[\mu mol/m^3(air)]$; the EQSAM4clim computations (see Sec. S2) are performed in $[mol/m^3(air)]$. For comparison with SP2006, we use ppbv. Units, e.g., in $[\mu mol/m^3(air)]$ can be converted to ppbv by multiplication with the molar volume 24.465 $[L/mol]$, and from $[\mu g/m^3(air)]$ by additional division with the compounds molar mass, M_s.

At T_o = 298.15 K, P_o = 1 atm and RH = 50 % (i.e., $RH < RHD_{AN}$), with M_s in units of $[g/mol]$ (and 1 ppbv = 1 nano Liter gas per 1 Liter air = 1 micro Liter(gas) per m^3(air)), the unit conversion to $[ppbv]$ from concentrations in $[\mu g(gas)/m^3(air)]$ yields, e.g., for NH_3(g)=17.04 and HNO_3(g)=63.02 (see example on p474 of SP2006):

- NH_3(g) :17.04 $[\mu g(gas)/m^3(air)]$/17.04 $[g/mol]$·24.465 $[L/mol]$ = 24.465 [ppbv]
- HNO_3(g):63.02 $[\mu g(gas)/m^3(air)]$/63.02 $[g/mol]$·24.465 $[L/mol]$ = 24.465 [ppbv]

The partial pressure product is $24.465^2 \approx 600$ $[ppbv^2]$ and at this T well above the equilibrium value of $K_{p,AN}(T) = 57.5$ $[ppbv^2]$ (Table 4; Fig. 1), but lower than the value of 655 $[ppbv^2]$ given in SP2006, which corresponds to $T = 308$ $[K]$.

Following SP2006 for this dry case, the amount x $[ppbv]$ of the gaseous concentration C_i $[ppbv]$, which could form a solid, can be directly computed by solving the equation:

$$\prod_{i=1}^{n}(C_i - x) = K_p(T) \tag{S1}$$

For ammonium nitrate, (R1) yields a quadratic equation (with $a \cdot x^2 - 2 \cdot b \cdot x + c = 0$) $(24.5 - x)(24.5 - x) = 57.5$ $[ppbv^2]$, i.e., $x^2 - 49x + 543 = 0$. And, upon solving (with $x_{1,2} = 0.5 \cdot (-b \pm \sqrt{(b^2 - 4 \cdot a \cdot c)})/a$), i.e.,: $x_1 = 0.5 \cdot (49 - \sqrt{(2401 - 4 \cdot 543)}) \approx 16.9[ppbv]$. Note that the second solution ($x_2 \approx 32.1$) is to be discarded, since its value is larger than the actual C_i concentrations. Thus, an equal amount of 16.9 $[ppbv]$ of each NH_3(g) and HNO_3(g) and solid NH_4NO_3(s) would be in equilbrium at this temperature and RH. In terms of mass loadings, this corresponds to 11.8 and 43.5 and 55.2 $[\mu g/m^3(air)]$, respectively. The mass loadings of the corresponding residual (free) acids are: NH_3(g)= $(24.5 - 16.9)/24.5 \cdot 17 = 5.3$ and HNO_3(g)= $(24.5 - 16.9)/24.5 \cdot 63 = 19.5$ $[\mu g/m^3(air)]$, respectively. This case is illustrated in Fig. 3 (see upper panels); Sec. 2.4.1 and 2.5.

S1.2 Pure NH_4NO_3–gas-liquid equilibrium ($RH \geq RHD$)

Same as the first example, but with $RH = 80$ % and above the RHD_{AN}. In line with the dry case (Sec. 2.4.1 and S1.1), the amount x [*ppbv*] of the gaseous concentration C_i [*ppbv*], which could form aqueous ammonium nitrate, can be directly computed with Eqs. (6–12), if Eqs. (2–3) are used to solve $\mathrm{K}_p(T, RH)$ (see Sec. 2.4.2). Then, (R-1) can be analogously solved by using Eq. (S1) of the above dry case (Sec. S1.1):

$$\prod_{i=1}^{n}(C_i - x) = K_p(T, RH) \tag{S2}$$

For instance, considering the gas-aqueous phase equilibrium of ammonium nitrate at $RH = 80$ %, by assuming that the water activity a_w equals $RH/100$, we can obtain a value of 10 $[mol_{AN}/kg(H_2O)]$ of the corresponding solute molality, $\mu_{AN}(a_w = 0.8)$, from measurements, or from Eq. (A3) of Sec. A2; both are shown in Fig. A1 (in Sec. B). Using Eq. (S2), with $M_s = 0.08$ $[kg/mol]$ (of Table 1), we find for the solute mass fraction (using Eq. A1) the corresponding value of: $\chi_{AN}(a_w = 0.8)$=$(\frac{1}{0.08\cdot 10}$+$1)^{-1}$= 0.44. And from Eq. (3) we obtain, $COEF_{AN}(RH = 80\%) = 2{\cdot}0.44^2$= 0.39, so that we can directly obtain the required value for the T– and RH–dependent ammonium nitrate equilibrium dissociation constant from Eq. (S2). At $T = 298$ (using the value given in Table 4) we accordingly find $K_{p,AN}(T = 298, RH = 80\%)$ =57.5·0.39 $\approx$ 22 $[ppbv^2]$.

Mozurkewich (1993) gives a $K_p^o(T_o)$ value of 42 $[ppbv^2]$, for which we would obtain at RH=80%, 41.9·0.39 $\approx$ 16 $[ppbv^2]$ and accordingly $\approx$ 12 $[ppbv^2]$ for the value 29.9 $[ppbv^2]$, which was originally given by Pilinis and Seinfeld (1987) (e.g., for use in the thermodynamic model SEQUILIB). For EQSAM4clim, either $K_p^o(T_o)$ value can be used. The corresponding value of SP2006 (given in their example below Eq. (10.99)) is $\approx$ 15 $[ppbv^2]$.

Thus, knowing $K_{p,AN}(T, RH)$ one can directly solve the quadratic equation Eq. (S2) for the aqueous phase analogously to Eq. (S1) for the dry case, without any iterations. Using $K_{p,AN}(T = 298, RH = 80\%) \approx 22$ $[ppbv^2]$ and the gas concentration for the solid example given for Eq. (S1), we obtain for the equilibrium concentrations at RH=80%: $(24.5 - x)(24.5 - x) = 57.5{\cdot}0.39 \approx 22$, i.e., $x^2 - 49x + 578 = 0$. And, upon solving the quadratic equation $x_1 = 0.5 \cdot (49 - \sqrt{(2401 - 4 \cdot 578)}) = 19.8$ [*ppbv*] (the second solution has to be discarded, since its value is always larger than the actual C_i concentrations). Using $K_{p,AN}(T = 298, RH = 80\%)$ $\approx$16 $[ppbv^2]$ yields = 20.5 [*ppbv*], while using the ppb values of the example of SP2006 gives $(5 - x)(6 - x) = 15$, i.e., $x^2 - 11x + 15 = 0$, which yields $x_1 = 0.5{\cdot}(11 - \sqrt{(121 - 4 \cdot 15)}) = 1.6$ [*ppbv*]. Thus, an equal amount 19.8 (20.5, 1.6) [*ppbv*] of each NH_3(g) and HNO_3(g) and aqueous NH_4NO_3(aq) would be in equilbrium at this temperature and RH. The corresponding mass loadings of the residual (free) acids are: $(24.5 - 19.8)/24.5 \cdot 17 = 3.3$ and $(4.7)/24.5 \cdot 63 = 12.1$ $[\mu g/m^3(air)]$, respectively, and those of the aqueous cation and anion are: $NH_4{}^+$(aq)= $19.8/24.5 \cdot 18 = 14.6$, and $NO_3{}^-$(aq)= $19.8/24.5 {\cdot} 62 = 50.1$ $[\mu g/m^3(air)]$. The sum, $14.6 + 50.1 = 64.7$ $[\mu g/m^3(air)]$ forms NH_4NO_3(aq) and would be in equilibrium with NH_3(g)=17.04 and HNO_3(g)=63.02 $[\mu g/m^3(air)]$ at $T = 298.15$ $[K]$ and $RH = 80$ [%], while respectively 3.3 and 12.1 $[\mu g/m^3(air)]$ of NH_3(g) and HNO_3(g) remain in the gas phase.

Compared to the solid case, the additional formation of $64.7 - 55.2 \approx 9.5$ $[\mu g/m^3(air)]$ NH_4NO_3 corresponds to a change in RH from 50 to 80 [%]. Fig. 10.21 of SP2006 depicts the situation of the RH-dependent equilibrium partitioning. For comparison Fig. 2 (see line-points) and Fig. 3 (left part of the upper panels) reveals the situation for our EQSAM4clim and the ISORROPIA II applications.

S1.3 EQSAM4clim algorithm: NH_4NO_3–equilibrium

To provide a complete example for mixed solution cases with an analytical solution of EQSAM4clim (Sec. 2.5), we consider Fig. 3 (Sec. S1.1–S1.2) in terms of the notation of SP2006. For EQSAM4clim, we obtain the $NH_4NO_{3(nro)}$ equilibrium concentration by solving Eqs. (6–12), based on chemical domains (Table 2, Sec. 2.2) and the neutralization reaction order (NRO, Table 3, Sec. 2.3).

I. Single Solution, Dry/Wet Case (Fig. 3, upper panels)

For the single solution case shown in Fig. 3, we assume for the EQSAM4clim computations a total (gas+aerosol) cation and anion input concentration of 1 $[\mu mol/m^3(air)]$, i.e., total ammonium $[TA] = [NH_4^+]_{(nro,free)} = 1$ and total nitrate $[TN] = [NO_3^-]_{(nro,free)} = 1$. For this sulfate neutral case (all other ions are zero), we apply domain D1. Solving the NRO for D1 automatically yields only a single reaction, i.e., for NH_4NO_3, since all other cation and anion products are zero, so that just one ion-pair combination can exist. Considering the ion charge, $[ZN] = [ZA] = 1$, we can obtain from the product $[TA] \cdot [ZA]$ and $[TN] \cdot [ZN]$ the corresponding maximum ammonium nitrate concentration $[NH_4NO_{3(nro,max)}] := MIN([TA] \cdot [ZA], [TN] \cdot [ZN]) = 1$ $[\mu mol/m^3(air)]$, which is possible for the input concentration with $K_p(T, RH, Y) := 1$ (Sec. 2.5), T and RH. The temperature is fixed to $T = 298.15$ K, the RH varies from $RH = 30$ to $RH = 100$ [%]. After solving the NRO, [TA] and [TN] are zero over the entire RH–range, since here the input concentrations are fixed to 1 $[\mu mol/m^3(air)]$ for this pure NH_4NO_3 case (binary solution, upper left panel of Fig. 3). To solve a dry and wet case, we again consider $RH = 50$ [%] and $RH = 80$ [%]. According to Table 1, the RHD= 61.83 [%] for NH_4NO_3 so that at $RH = 50$ [%] only the gas-solid equilibrium partitioning needs to be considered, i.e., (R1), while at $RH = 80$ [%] the gas-liquid equilibrium partitioning, i.e., (R2), is relevant. In EQSAM4clim we solve the equilibrium in molal scale. At $T = 298.15$ K and $RH = 50$ [%], conversion of $K_p(T) = 57.46$ $[ppbv^2]$ (Table 4) to the molal scale yields (with $K_p/(RT/P)^2$), i.e., 57.46 $[ppbv^2]$ $\cdot 10^{-18}/(8.314409/101325$ $[m^3(air)/mol/K] \cdot 298.15$ $[K])^2 = 57.46 \cdot 1.67^{-15} = 9.6 \cdot 10^{-14}$ $[mol/m^3(air)]^2$. Solving Eqs. (6–12), we then obtain for the evaporative loss $[x]$ $[\mu mol/m^3(air)]$ of $[NH_4NO_{3(nro,max)}]$:

$x = 0.5 \cdot \sqrt{(4 \cdot 9.6 \cdot 10^{-14})} = 0.31$ $[\mu mol/m^3(air)]$, with $[TA] = [TN] = 0$. Thus, at $RH = 50$ [%], $NH_4NO_{3(s,nro)} = 1 - 0.31 \approx 0.69$ $[\mu mol/m^3(air)]$, or $0.69[\mu mol/m^3(air)]$ $\cdot$ 80 $[g/mol] \approx 55.2$ $[\mu g/m^3(air)]$ for the total particulate matter (PM). For the aqueous phase at $RH = 80$ [%], we analogously obtain $NH_4NO_{3(aq,nro)}$. According to the above example (Sec. S1.2), $K_{p,AN}$ $(T = 298, RH = 80\%)$ =57.5·0.39 ≈ 22 $[ppbv^2]$, so that we get; $= 22 \cdot 1.67^{-15} = 3.7 \cdot 10^{-14}[mol/m^3(air)]^2$ and $x = 0.5 \cdot \sqrt{(4 \cdot 3.7 \cdot 10^{-14})}$ ≈ 0.19 $[\mu mol/m^3(air)]$. This yields $NH_4NO_{3(aq,nro)} \approx 0.81$ $[\mu mol/m^3(air)]$, or for the total PM ≈ 0.81 $[\mu mol/m^3(air)]$ $\cdot$ $80[g/mol] \approx 64.6$ $[\mu g/m^3(air)]$. These values refer respectively to the (upper) left and right panels of Fig. 3, and are close to the values of ISORROPIA II, which are independently computed with a different approach.

II. Mixed Solution, Dry/Wet Case (Fig. 3, lower panels)

For the mixed solution case shown in Fig. 3, we assume for the EQSAM4clim computations a total (gas+aerosol) cation and anion input concentration ($[\mu mol/m^3(air)]$)

of total ammonium $[TA] = [NH_4^+]_{(nro,free)} = 3$, total nitrate $[TN] = [NO_3^-]_{(nro,free)} = 1$, and total sulfate $[TS] = [SO_4^{2-}]_{(nro,free)} = 1$. This sulfate case also falls into domain D1, since other ions are zero. Solving the NRO for D1 yields two reactions. Considering the ion charge, $[ZN] = [ZA] = 1$ and $[ZS] = 2$, we can directly obtain from the NRO and the products $[TA] \cdot [ZA]$, $[TN] \cdot [ZN]$ and $[TS] \cdot [ZS]$ the corresponding maximum concentrations of ammonium sulfate and ammonium nitrate, which is possible for the input concentration with $K_p(T, RH, Y) := 1$ (Sec. 2.5 and S1.3-I):

1. $[TA] \cdot [ZA] = 3$ and $[TS] \cdot [ZS] = 2$:
   $[(NH_4)_2SO_{4(nro,max)}] := MIN([3], [2]) = 1$

2. $[TA = 3 - 2 = 1] \cdot [ZA = 1] = 1$ and $[TN = 1] \cdot [ZN = 1] = 1$:
   $[NH_4NO_{3(nro,max)}] := MIN([1], [1]) = 1$

Extending our above example calculation (Sec. S1.3-I) to the mixture of NH_4NO_3 of 1 $[\mu mol/m^3(air)]$ of each NH_4NO_3 and $(NH_4)_2SO_4$ (lower left panel of Fig. 3), we compute the dry ($RH = 50$ [%]) and wet ($RH = 80$ [%]) case. For NH_4NO_3, the RHD= 61.83 [%] and for $(NH_4)_2SO_4$ the RHD= 79.97 [%] (Table 1), so that at $RH = 50$ [%] again only the gas-solid equilibrium partitioning needs to be considered. Note that mixed solution effects described in Sec. 2.6 are not considered for the RHD in this example, but they are considered for the gas-liquid and liquid-solid equilibrium partitioning and associated aerosol water uptake examples presented in Sec. 3.

For the mixed solution case, the computation is similar to that discussed above (Sec. S1.3-I), only the ionic strength factor needs to be included for the wet case. For the dry case, the solid equilibrium concentration, $NH_4NO_{3(s,nro)}$, is identical, since $Y := 1$ (the ionic strength correction factor is defined only for solutions). The total dry aerosol mass therefore is the sum of the $NH_4NO_{3(s,nro)}$ (from above) and $(NH_4)_2SO_{4(s,nro)}$ masses, i.e., PM $\approx 55.2 + 132.2 = 187.4$ $[\mu g/m^3(air)]$. For the aqueous case, we obtain Y from Eq. (4) (as used for Eq. 5), i.e., we obtain for 1 $[\mu mol/m^3(air)]$ of each, $NH_4NO_{3(aq,max,nro)}$ and $(NH_4)_2SO_{4(aq,eq)}$, $Y = \frac{1}{1+3\cdot 1} = 0.25$. Using further the above (Sec. S1.2) value for $\mu_{AN}(a_w = 0.8) \approx 10$ $[mol_{AN}/kg(H_2O)]$ (Fig. A1), we compute the solute mass fraction again from Eq. (A1) as $\chi_{AN}(a_w = 0.8) = (\frac{1}{0.08\cdot 10} + 1)^{-1} = 0.44$. Then, Eqs. (3) and (5) yield $COEF(RH, Y) = 2 \cdot 0.44^2 \approx 0.39$ and $Y^{0.8} = 0.25^{0.8} = 0.33$, so that $K_{p,AN}(T = 298, RH = 80\%, Y = 0.25) = 57.5 \cdot 0.39 \cdot 0.33 = 7.4$ $[ppbv^2]$, or $7.4 \cdot 1.67^{-15} = 1.24 \cdot 10^{-14}$ $[mol/m^3(air)]^2$. Solving Eqs. (6–12), we then again obtain for the evaporative loss $[x]$ $[\mu mol/m^3(air)]$ of $[NH_4NO_{3(nro,max)}]$:

$x = 0.5 \cdot \sqrt{(4 \cdot 1.24 \cdot 10^{-14})} \approx 0.11$ $[\mu mol/m^3(air)]$, with $[TA] = [TN] = 0$. Thus, at $RH = 80$ [%], $NH_4NO_{3(aq,nro)} = 1 - 0.11 \approx 0.89$ $[\mu mol/m^3(air)]$, or for the total (dissolved) PM ≈ 0.89 $[\mu mol/m^3(air)] \cdot 80 [g/mol] + 132.2 [\mu g/m^3(air)] = 203.4$ $[\mu g/m^3(air)]$. These values refer to the (lower) left and right panels of Fig. 3, respectively, and are also close to the results of ISORROPIA II, despite the distinctly different approaches.

S2 Computational algorithm of EQSAM4clim

The EQSAM4clim computational algorithm is summarized as follows (see Fig. S2.2-S1):

- EQSAM4clim (v09), described in Sec. B, considers the salt compounds listed in Table 1. To calculate the gas-liquid-solid partitioning, a pre-calculated (constant) ν_i

coefficient is used for each compound (ion-pair), which is obtained from a small set of thermodynamic data: stoichiometric coefficient ν_s $[-]$, the ion-pair charge Z_s $[-]$, the single solute parameter ν_i $[-]$, the mass fraction solubility W_s $[\%]$, the molar mass M_s $[kg/mol]$, the density D_s $[kg/m^3]$, the RHD(T_o) $[-]$ at reference temperature $T_o = 298.15$ $[K]$ and the corresponding temperature coefficients, $T_{coef(RHD)}$ $[-]$. For all salt compounds, ν_i has been pre-determined with the bi-section method by the procedure of solving Eq. (5b) of M2012 (Eq. A6 in Appendix A4), using measurements of W_s–RHD(T_o) (single data pairs) at T_o, which are listed with ν_i in Table 1. The required RHD values, including T-coefficients, have been taken from ISORROPIA II for a consistent comparison (Fountoukis and Nenes, 2007). All other data of Table 1 have been taken from the CRC Handbook of Chemistry and Physics (2006).

- The EQSAM4clim algorithm starts with the assignment of two internal loop parameters: An outermost loop, considering e.g., vertical model levels, and an innermost vector loop for e.g., the longitude–latitude grid box that contains the input-data for a given time-step. Both loops are scalable and can be externally determined depending on the climate model set-up, e.g., to best match the cache of the compute nodes. The consideration is optional and can be controlled in the subroutine call. The actual computations are structured in blocks, which are fully sequential. Each computational block has its own vector loop with the compound specific logic around it, so that loops can be fully optimized by the compiler and iterations between different computational blocks are avoided. All computational blocks are within an outermost loop (for this version).

- The first two computational blocks (out of 15) assign the T $[K]$ and RH $[0-1]$ data, as well as the lumped cations and anion concentrations $[mol/m^3(air)]$. Further, the total cation and anion concentration charge is computed and a logical switch for each compound is defined. Thus, we assume that a compound can be formed only, if the product of the required cation and anion concentration is non-zero. This compound specific flag is subsequently used to skip the computation of individual compounds, which may not be present at the considered model time step. The flag is applied to all computational blocks which have an outer compound loop. In case all cation and anion concentrations are zero, i.e., the total cation charge equals (or is below) REALZERO = tiny(0._dp) (with dp = SELECTED_REAL_KIND(12,307)), none of the compounds could form and we therefore skip all computations. Depending on the EMAC model set-up and the number of compounds considered, this may happen for instance in remote locations such as the upper stratosphere. Both options are merely included to minimize the overall computational burden.

- To further minimize the CPU time, the next computational block (3) defines:
  - Whether solids are excluded or included, i.e., the hysteresis loop. The criteria depend on the presence of aerosol water of the previous time step. In case aerosol water is not present, the aerosol is assumed to be dry and the water uptake is calculated based on RH and RHD thresholds. Otherwise, gas-liquid partitioning is considered and the water uptake is calculated without RHD thresholds, assuming the aerosol phase to be metastable.
  - The domain that needs to be considered. Similar to ISORROPIA II, we consider a domain approach (Sec. 2.2). But the approach used here only depends

on the input concentration ratio of total cations (tCAT) to total sulfate anions (tSO_4), which is more elementary compared to the domain approach used in ISORROPIA II and is similar to the one used in the original EQSAM code (Metzger et al., 2002). Table 2 lists the domains used to characterize the potential sulfate aerosol neutralization levels.

- The next two computational blocks initialize the internal arrays, including all output fields, while block (5) defines the neutralization reaction order for all compounds that may form for a given domain during the cation-anion neutralization. The compound's indices are ranked according to a preferred neutralization (from left to right). The domain dependent neutralization order is shown in Table 3.

- Computational block (6) solves the compound's solute molality μ_s from Eq. (A3), by optionally including the Kelvin-term. To avoid iteration, we take a two-step approach / approximation (see Appendix B):

  - Step one: $K_e = 1$, and $B = 0$ to obtain the initial μ_s from Eq. (A3).
  - Step two, repeated three times: μ_s from previous iteration is used to calculate K_e from Eq. (A7), χ_s from Eq. (A1), B from Eq. (A4). Then a new μ_s is obtained from Eq. (A3).

  Note that we sequentially solve the equations three times, whereby we only loop over those compounds of Table 1 that are allowed to form and those compounds that have a non-zero input ion-pair concentration (determined by block 2).

- The next computational block (7) calculates the temperature dependency of the RHD from Eq. (A5) and optionally considers the Kelvin effect according to Eq. (A7).

- In computational block 8, the actual cation-anion neutralization reactions are solved assuming chemical equilibrium. Based on the pre-defined reaction order the input cation and anion concentrations are balanced (neutralized) by looping over all compounds those cation-anion product is above REALZERO. As a result, the cation and anion concentrations subsequently decrease in favor of the concentrations of the corresponding compounds, independent of any solvent and solute activity.
  Within the same loop, we calculate the total solute activity and store the RHD values only for the compound's that have a non-zero concentration. This information is subsequently used to analytically solve the liquid-solid partitioning.

- Computational block 9 approximates the mixed solution RHD from Eqs. (18-21).

- Thus far, all compounds have been treated as non-volatile and are assumed to reside in the aqueous phase. Computational block (10) solves the gas-liquid or gas-solid partitioning for the two semi-volatile compounds, NH_4NO_3 and NH_4Cl, that may be present in the sulfate neutral / poor (D1) domain (Sec. 2.4). Within one loop, Eqs. (2-5) are computed and the reactions (Eq. R2) are sequently solved. In case the RH is below the semi-volatile compound's RHD, Eq. 1 is used.

- The liquid-solid partitioning is calculated for all salt compounds in computational block 11 from the weighted mixd solution approach, Eqs. (13-21), described in Sec. 2.6. Each compound is treated as solid (instantaneously precipitated from the solution) in case the RH is below the compound's RHD (binary solution), or in case of mixed solutions below the weighted RHD.

- Within computational block 12 all partial aerosol water mass are calculated from Eq. (22) for those compounds with a non-zero aqueous phase concentration. The total water mass is obtained from the sum of all partial water masses (Sec. 2.7).

- Computational block 13 estimates the final H^+ concentration $[mol]$ from the difference of the total anion and cation concentrations. Within EMAC/GMXe the H^+ concentration is recalculated for both EQSAM4clim and ISORROPIA II to account for the changes in the aerosol precursor gas concentrations, which may result from the size-dependent condensation of HNO_3, HCl and NH_3 and H_2SO_4 on the pre-existing aerosol surfaces (see Pringle et al., 2010a).

- Finally, the residual gases are calculated within computational block 14 from the remaining ion concentrations based on the implicit assumptions that: (i) Unneutralized ${NH_4}^+$ will instantaneously be fully vaporized to yield NH_3, unneutralized ${NO_3}^-$ yields HNO_3 and unneutralized Cl^- yields HCl. (ii) In addition, unneutralized ${SO_4}^{2-}$ is assumed to yield H_2SO_4, which is however treated as non-volatile; vaporization of H_2SO_4 is considered within GMXe (Brühl et al., 2012). H_2SO_4 contributes to the water uptake (assuming the solute molality of $(NH_4)_3H(SO_4)_2$).

- The last computational block (15) prepares the model output, which is user specific and can be individually extended or configured to write out all aerosol properties.

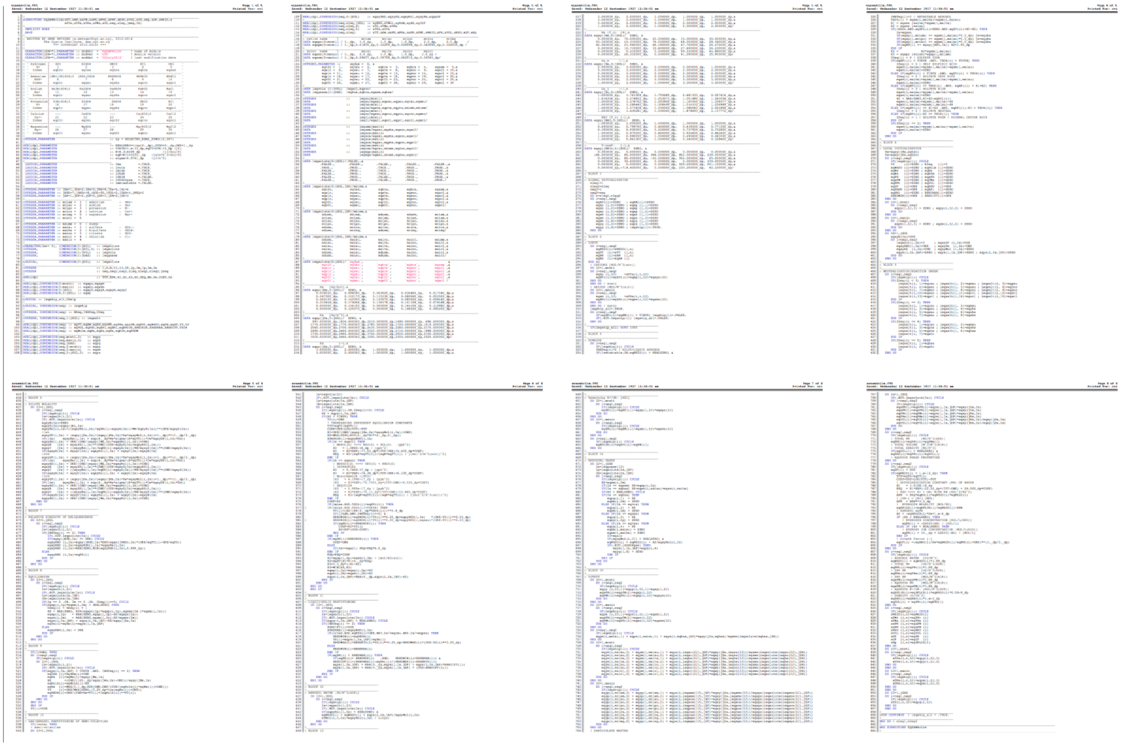

Figure S1: EQSAM4clim computational algorithm (code length overview, no details).

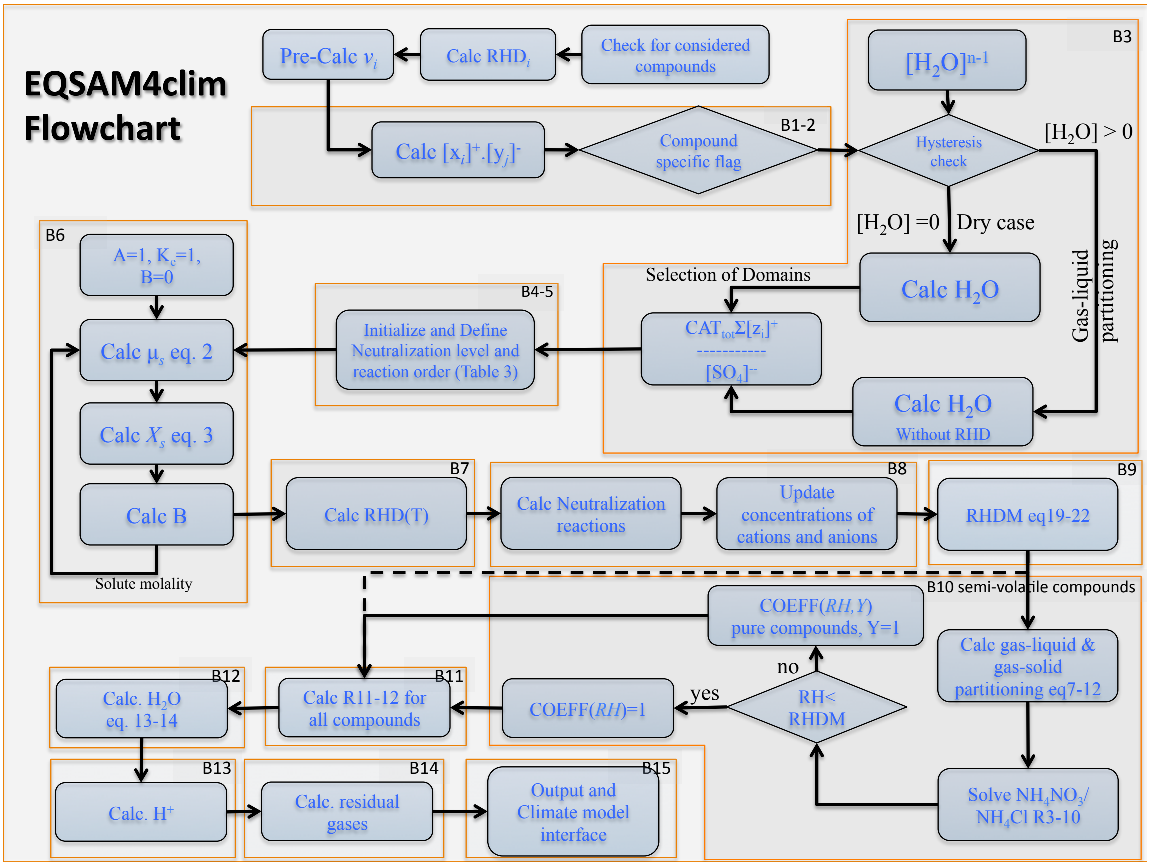

Figure S2.1: EQSAM4clim flowchart.

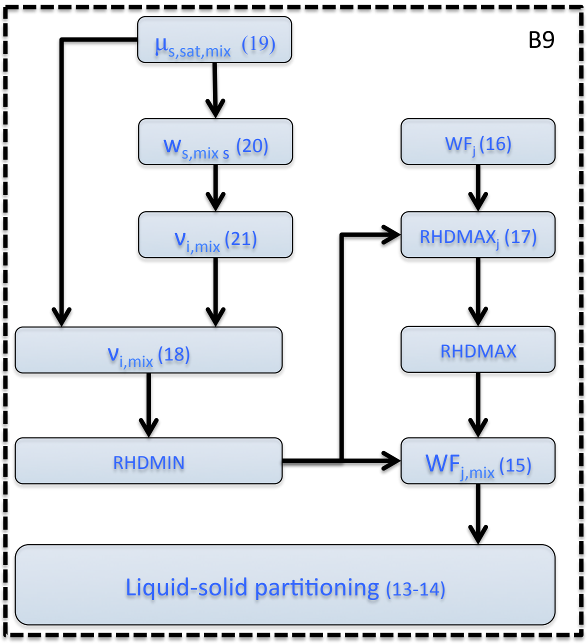

Figure S2.2: EQSAM4clim flowchart (B9): Calculation of mixed solution RHD (Sect. 2.6).

S3 Extended Applications

This section extends/complements the results shown in Sec. 3:

1. Fixed solute concentrations (9 cases): ISORROPIA II and E-AIM
   (see main text, Sec. 3.1)
2. Variable ammonia concentration: ISORROPIA II and Seinfeld and Pandis (2006)
   (see main text, Sec. 3.2)
3. Variable solute concentrations (20 cases): ISORROPIA II and EQUISOLV II
   (see main text, Sec. 3.3)
4. Field observations (MINOS campaign, 184 cases): ISORROPIA II
   (see main text, Sec. 3.4)

S3.1 Fixed solute concentrations

Figure S3 extends the aerosol water mass calculations shown in Figure 4 (see Sec. 3.1) to 9 binary and mixed solution cases with fixed aerosol concentrations. The results are based on the full gas-liquid-solid partitioning and compare the calculations of EQSAM4clim with ISORROPIA II and E-AIM, with each (dry) compound concentration fixed to 1 [$\mu mol/m^3(air)$]. The panels of Figure S3 show (from let to right, top-down):

- single solute solutions:
  (1.) NaCl; (2.) $(NH_4)_2SO_4$; (3.) NH_4NO_3;
- mixed solutions:
  (4.) NH_4HSO_4 / $(NH_4)_3H(SO_4)_2$;
  (5.) $NaHSO_4$ / $Na_3H(SO_4)_2$;
  (6.) NH_4NO_3 – $(NH_4)_2SO_4$;
  (7.) $NaNO_3$ – NaCl / NaCl;
  (8.) $(NH_4)_2SO_4$ – NH_4Cl – Na_2SO_4;
  (9.) NH_4NO_3 – $(NH_4)_2SO_4$ – NH_4Cl – Na_2SO_4

The large panels show the aerosol water mass predictions for the RH range $= 50 - 97$ [%], while the small inserted panels expand the range to RH $= 95 - 99.5$ [%].

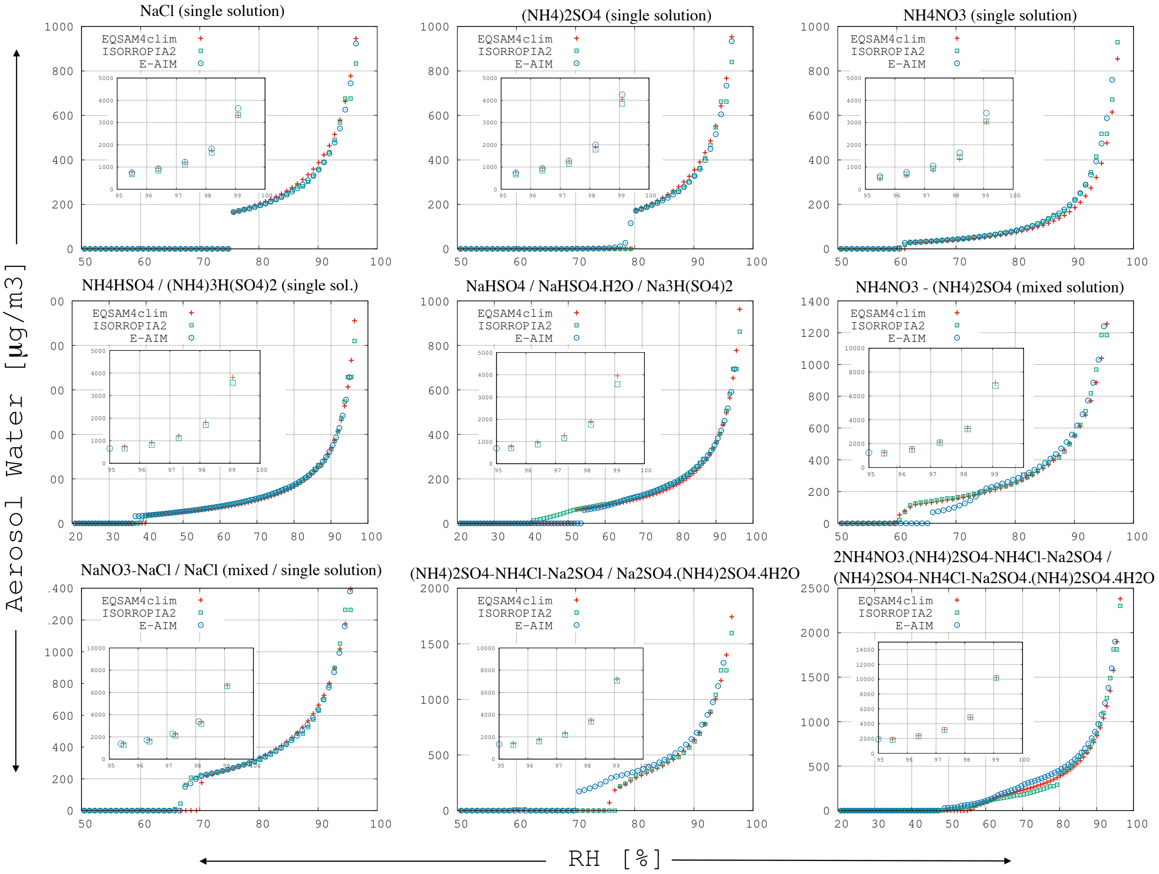

Figure S3: Extension of Figure 4 (main text): The bulk comparison of the total aerosol water mass, $m_{w,mix}$ $[kg/m^3(air)]$ obtained by Eq. (22) for EQSAM4clim, is shown for various single and mixed solutions. The dry concentration of each compound is fixed to 1 $[\mu mol/m^3(air)]$ at $T = 298.15\ K$. Results of EQSAM4clim (red crosses) and ISORROPIA II (green squares) are shown for $RH = 50 - 97$ [%] (large panels) and for the $RH = 95 - 99.5$ [%] (small panel). The results of E-AIM (web version) (blue circles) are included for comparison. The mixed solution RHD has been obtained for EQSAM4clim from Eq. (13–22) and are based on measured MDRH values for ISORROPIA II. The mutual deliquescence range of EQSAM4clim and ISORROPIA II (described in Sec. 2.6) differ from those of AIM (web version: $http://www.aim.env.uea.ac.uk/aim/aim.php$). Each panel is shown in the following for better reading.

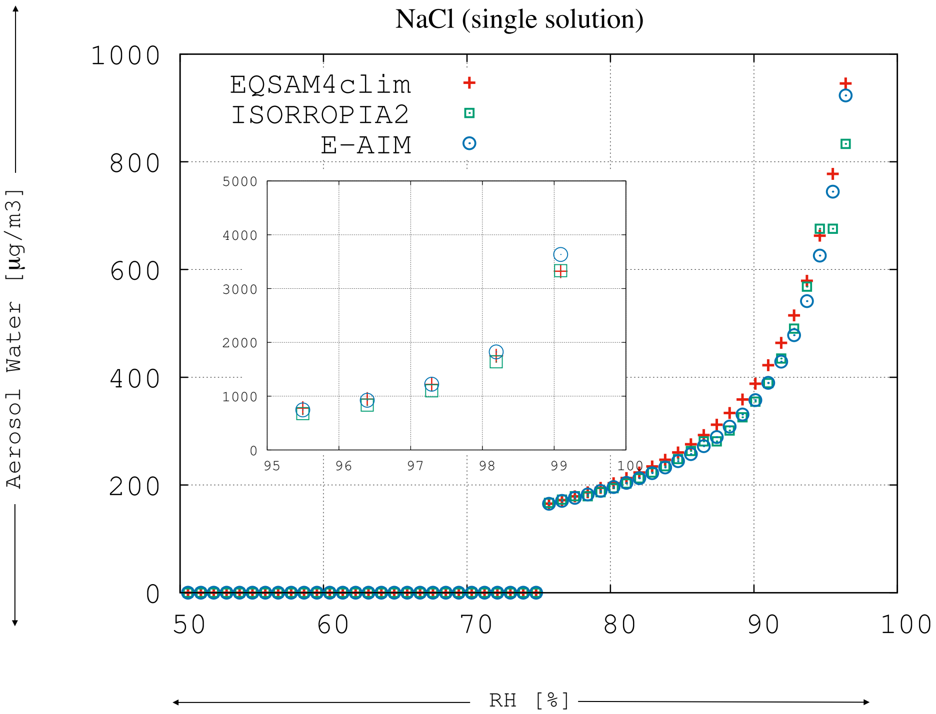

Figure S3.1: Panel 1 of Figure S3 (Supplement).

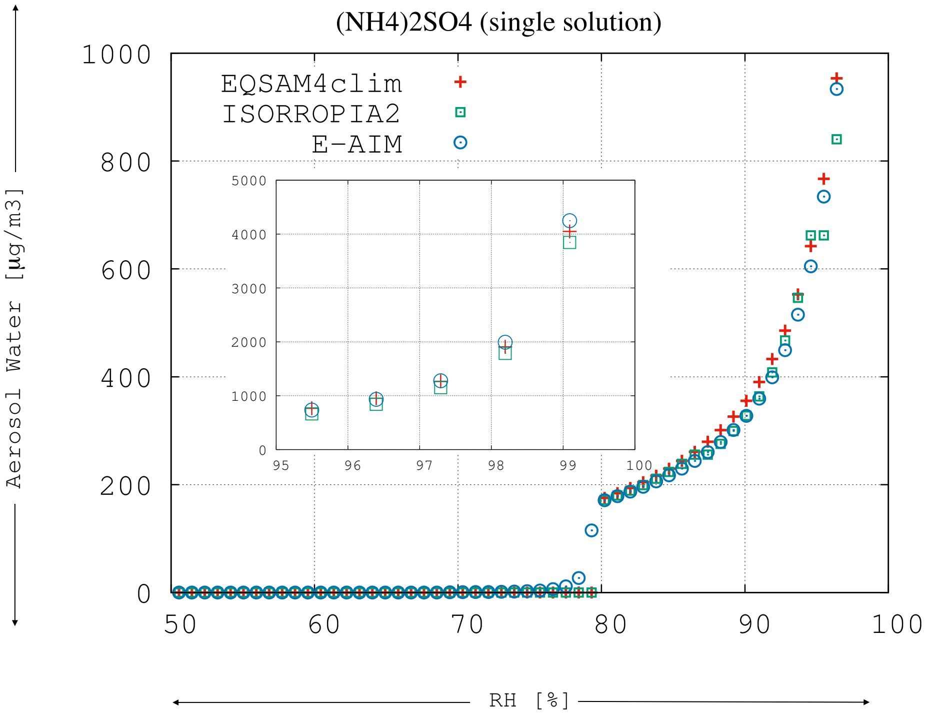

Figure S3.2: Panel 2 of Figure S3 (Supplement).

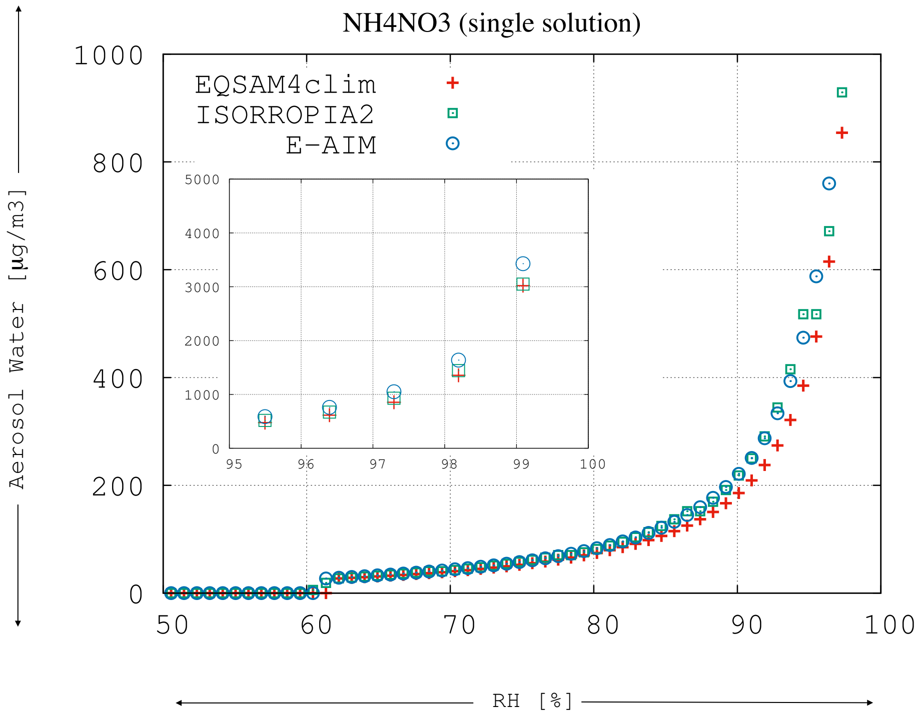

Figure S3.3: Panel 3 of Figure S3 (Supplement).

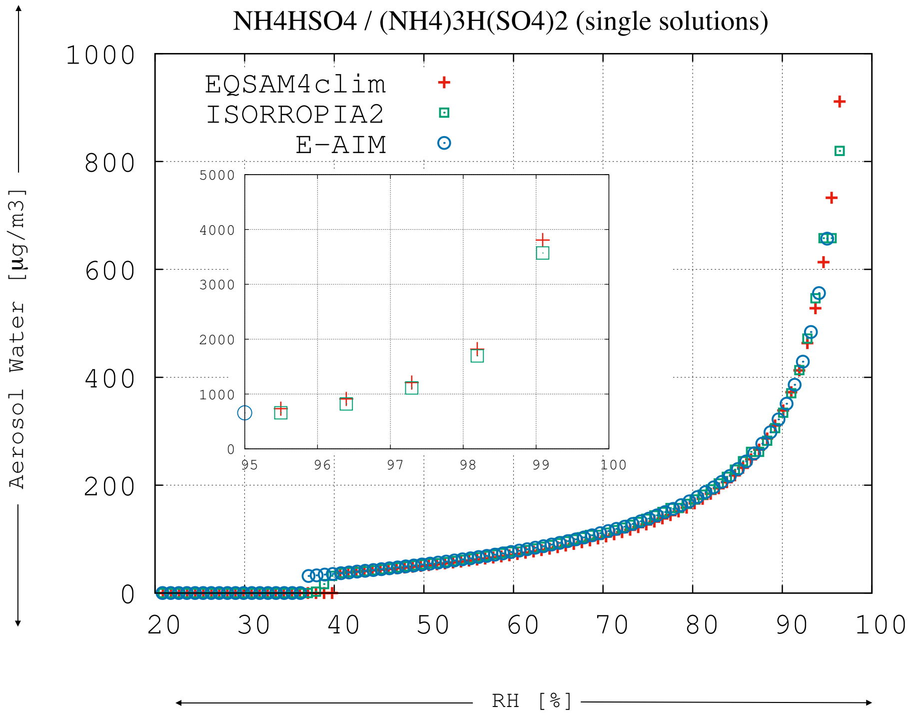

Figure S3.4: Panel 4 of Figure S3 (Supplement).

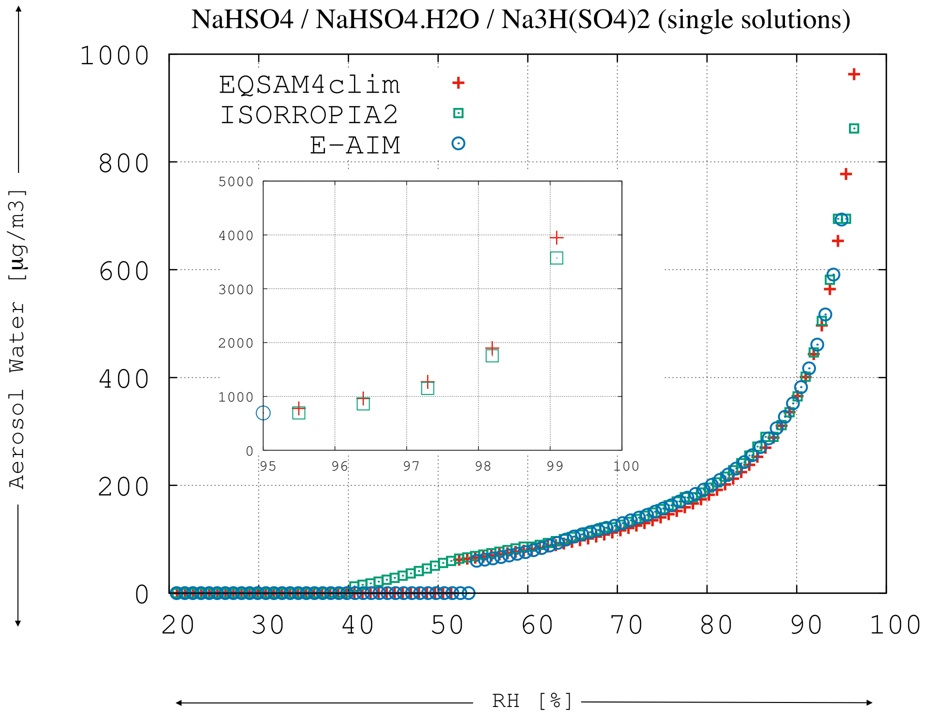

Figure S3.5: Panel 5 of Figure S3 (Supplement).

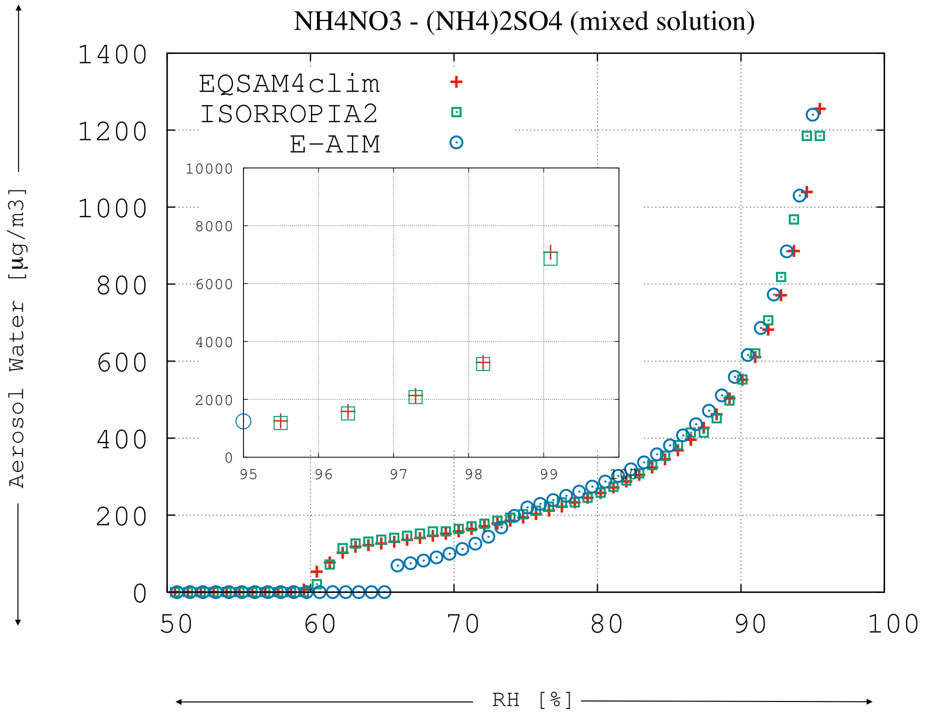

Figure S3.6: Panel 6 of Figure S3 (Supplement).

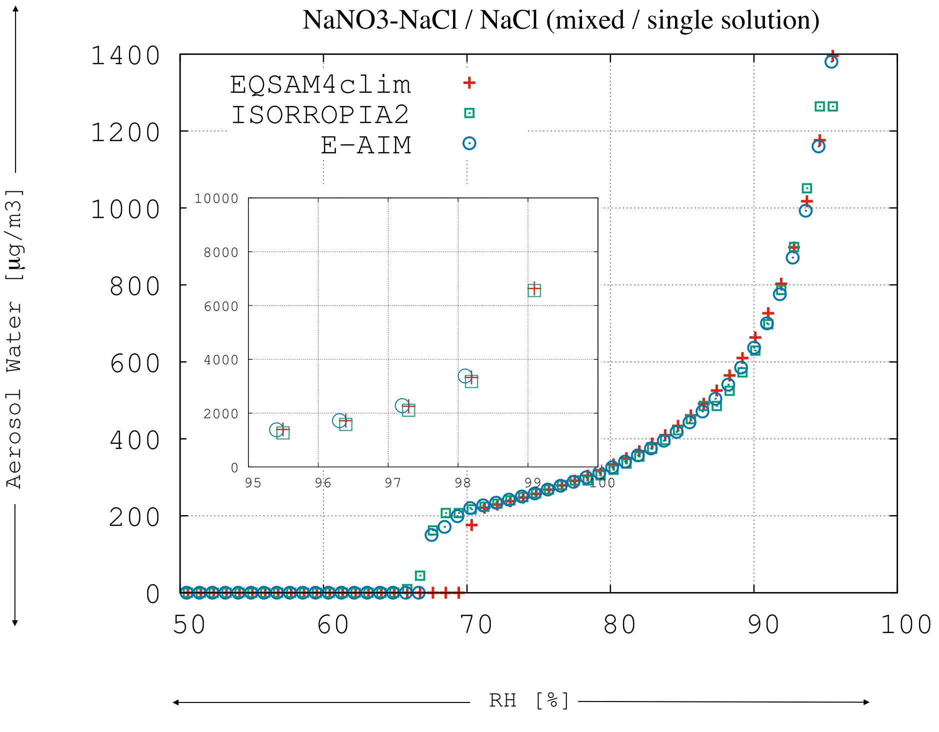

Figure S3.7: Panel 7 of Figure S3 (Supplement).

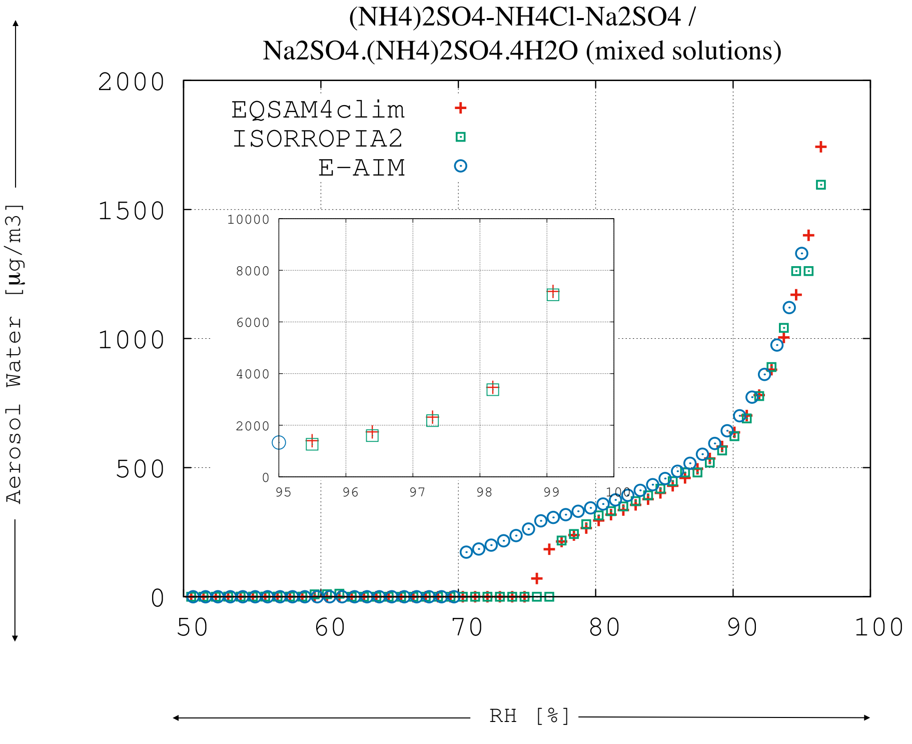

Figure S3.8: Panel 8 of Figure S3 (Supplement).

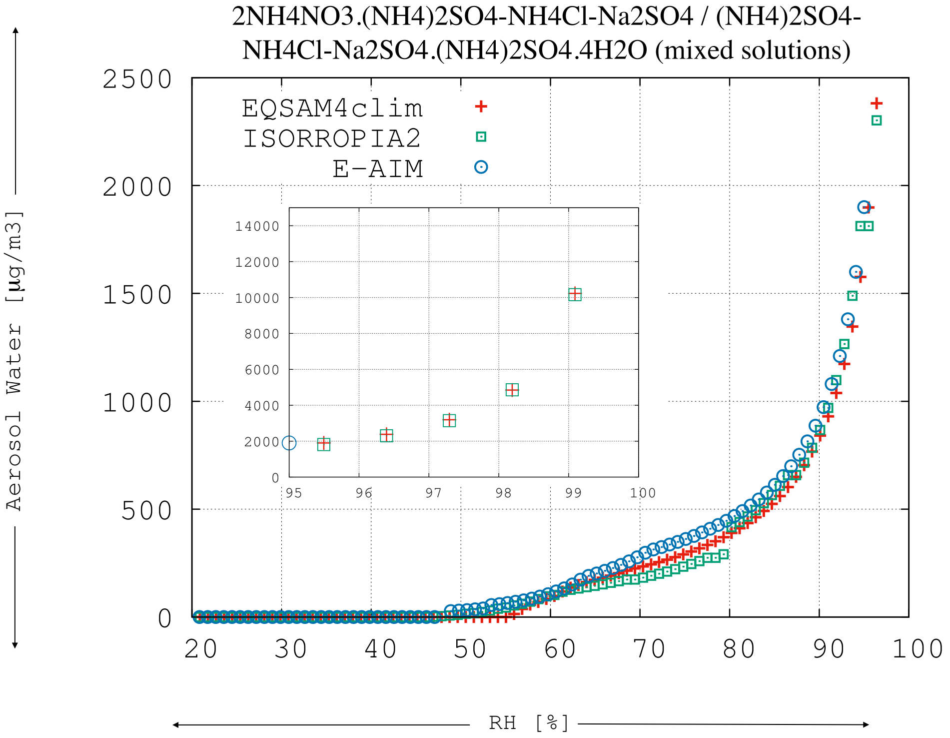

Figure S3.9: Panel 9 of Figure S3 (Supplement).

S3.2 Variable NH_3 concentration – SP2006

Figure S4 extends the Fig. 5 (main text) to bi-sulfate and sulfuric acid. Both, the gaseous uptake of NH_3 and HNO_3 on saturated solutions and the weak dissociation of, e.g., H_2SO_4 and HSO_4^-, are not considered for EQSAM4clim (see Sec. S2). Therefore differences occur for bi-sulfate, sulfate and water in the concentration range of ammonia, i.e., within $2 - 4$ [$\mu g/m^3(air)$]. At lower ammonia concentrations, where the sulfates are less neutralized, the bi-sulfate concentration increases and the sulfate concentration accordingly decreases, until only free sulfuric acid exists. Note that the differences between EQSAM4clim and ISORROPIA II are for ammonia concentrations below 2 [$\mu g/m^3(air)$] only a matter of naming definition – the version of ISORROPIA II used considers all unneutralized sulfate simply as sulfate, an output variable sulfuric acid does not exist, since sulfuric acid has such a low vapor pressure that it practically only exists in the aerosol phase. EQSAM4clim has an option to treat it either way.

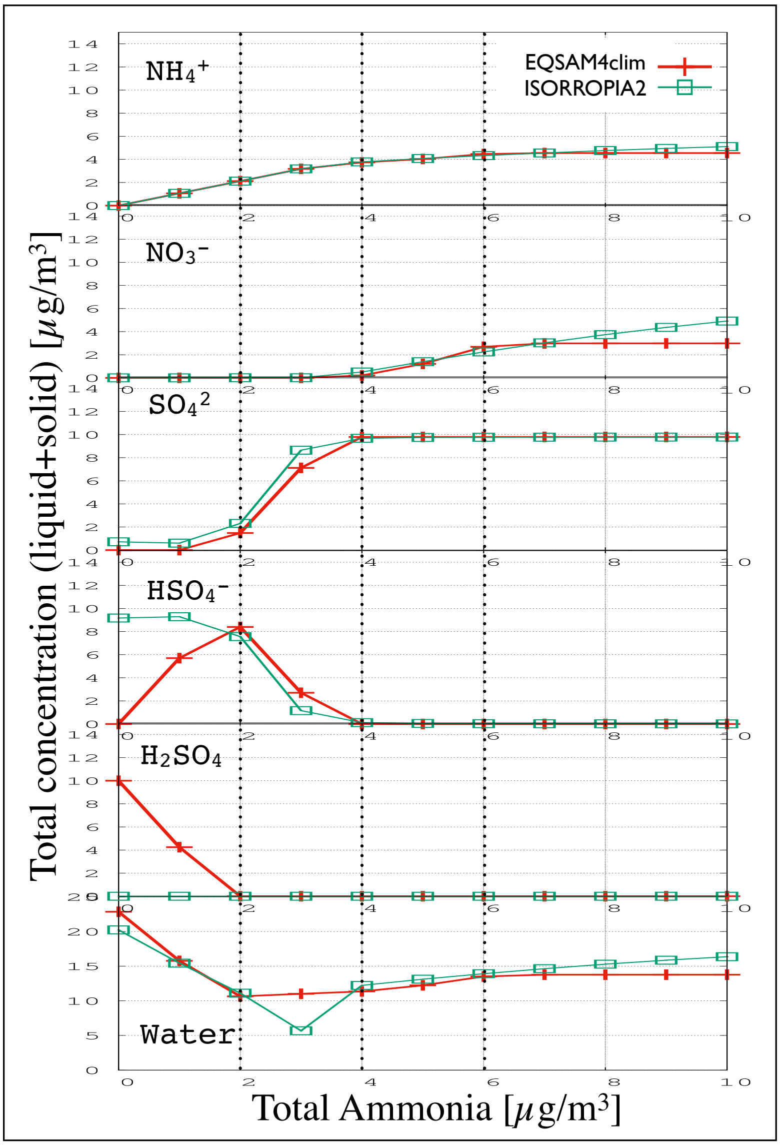

Figure S4: Extension of Figure 5 (main text): Mixed solution composition of NH_4NO_3 and $(NH_4)_2SO_4$ as a function of total ammonia at $T = 298.15$ $[K]$ and $RH = 70$ [%], as defined in SP2006 for their Figure 10.23. $[TS] = [TN] = 10$ $[\mu g/m^3(air)]$ showing EQSAM4clim (red crosses) and ISORROPIA II (green squares). Each panel is shown in the following for better reading.

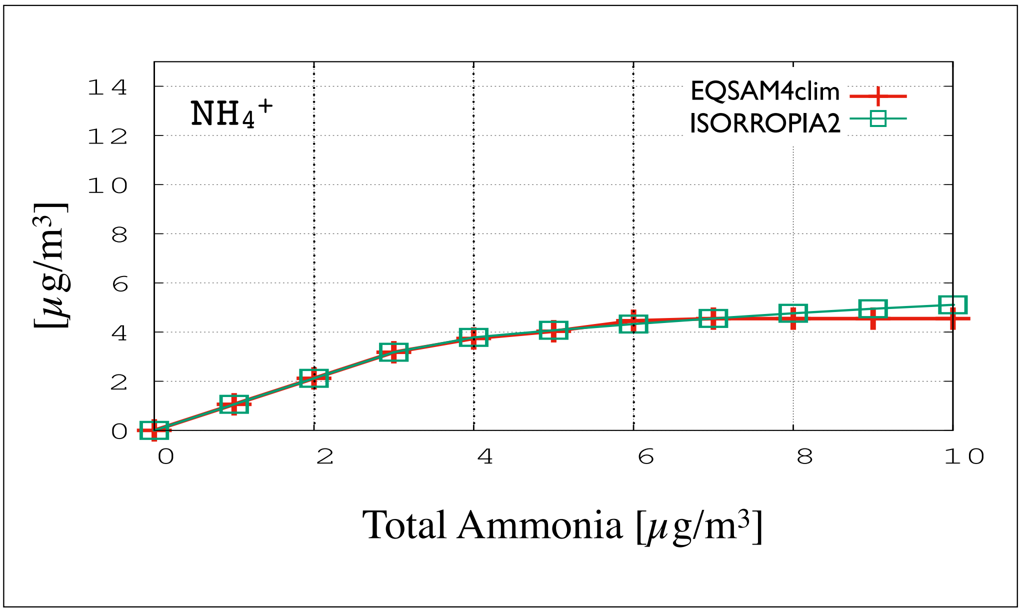

Figure S4.1: Panel 1 of Figure S4 (Supplement).

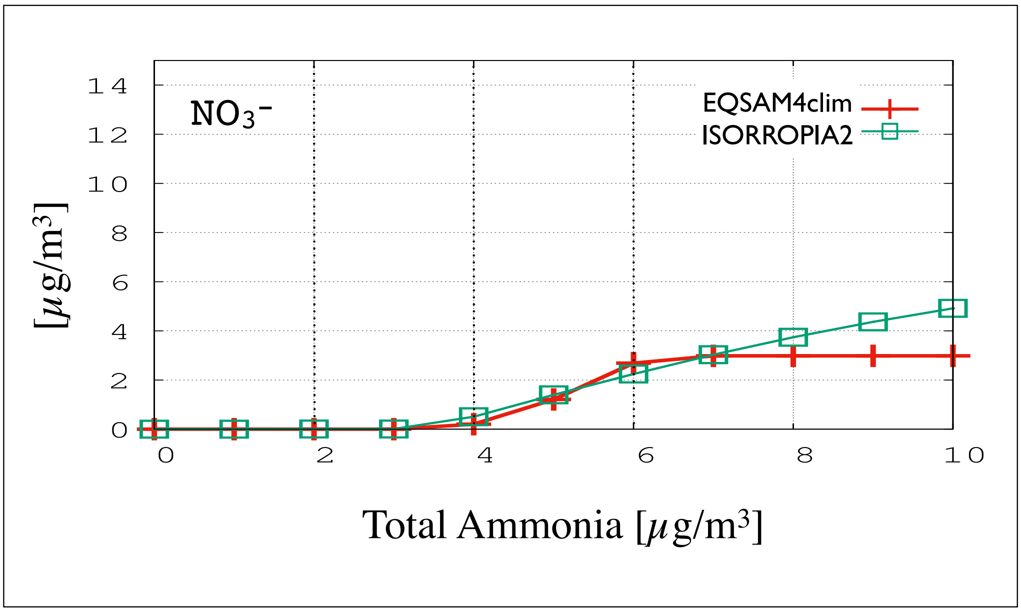

Figure S4.2: Panel 2 of Figure S4 (Supplement).

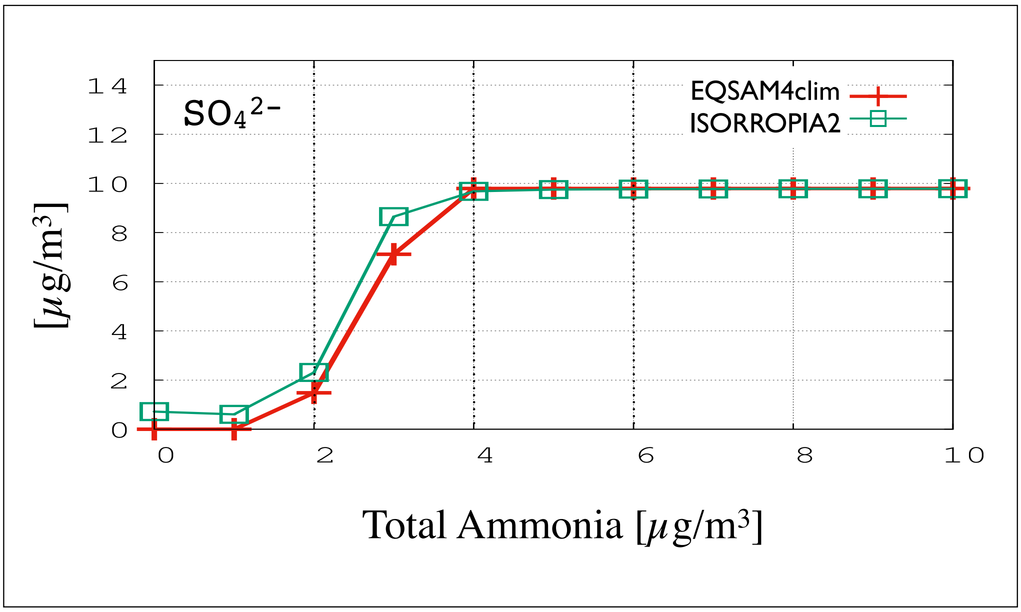

Figure S4.3: Panel 3 of Figure S4 (Supplement).

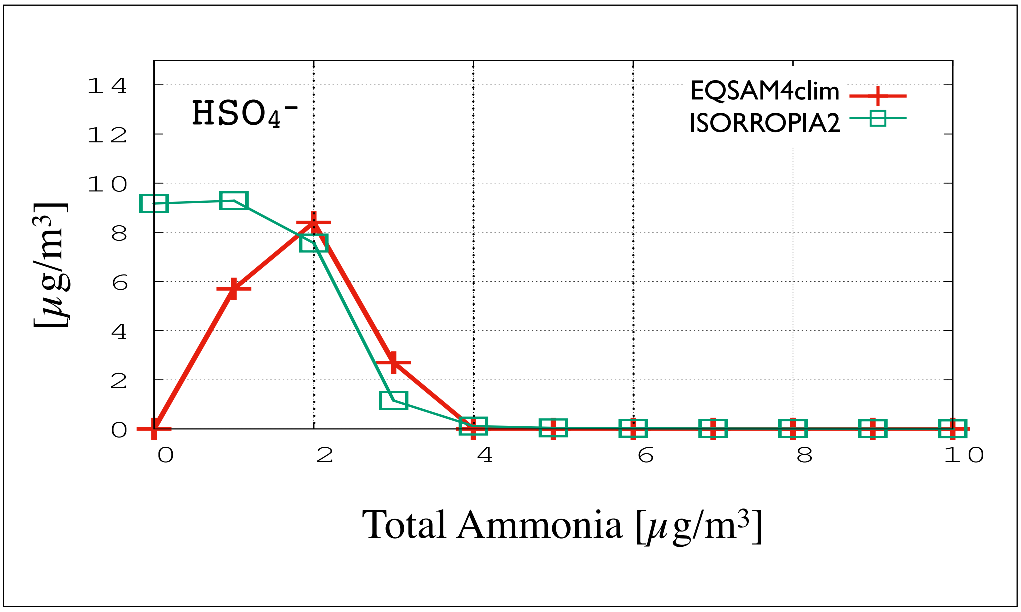

Figure S4.4: Panel 4 of Figure S4 (Supplement).

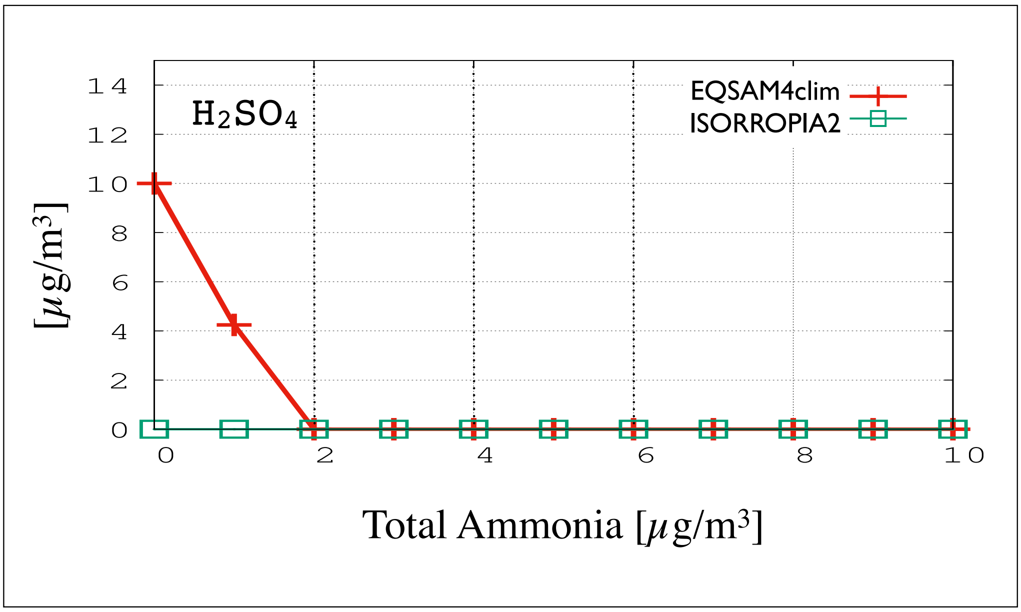

Figure S4.5: Panel 5 of Figure S4 (Supplement).

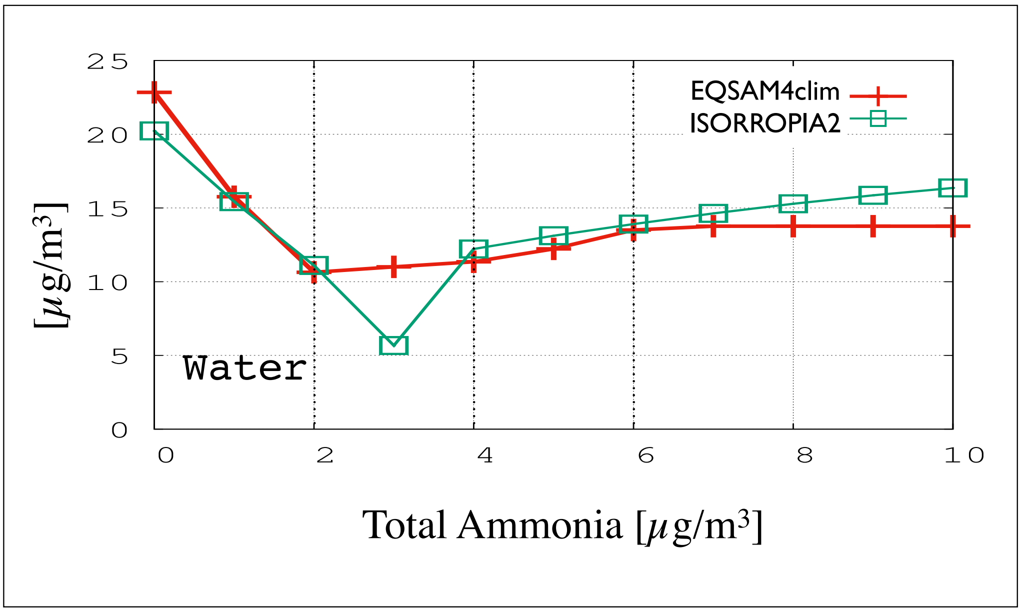

Figure S4.6: Panel 6 of Figure S4 (Supplement).

S3.3 Variable solute concentrations (20 cases)

Extension of Figure 6 and 7 to 20 aerosol composition cases. Cases 1–5 refer to the sulfate very rich regime, cases 6–10 to sulfate rich, and 11–20 to sulfate neutral and poor regimes (see Sec. 2.2). The concentrations of all aerosol components only depend on fixed molar ratios with respect to the total sulfate concentration, which is fixed to 20 $[\mu g/m^3(air)]$ for all 20 cases. The ratios are shown in Table 3 of Xu et al. (2009). Note that some of the cases are the same as in the model inter-comparison of Zhang et al. (2000), so that a direct comparison can be made to a wider range of equilibrium models, including AIM (the case number in the parenthesis in Table 3 of Xu et al., 2009, refers to the cases in the study by Zhang et al., 2000). Here, Figures S5–S7 show the corresponding results of EQSAM4clim, ISORROPIA II and EQUISOLV II for these 20 cases as a function of RH: $10, 20, 30, 40, 50, 60, 70, 80, 90, 95$ [%]. The aerosol composition is calculated for each model from the gas-liquid-solid equilibrium partitioning, assuming deliquescence.

Figure S5 shows for the cases 1-20 (from left to right and top to bottom), the bulk aerosol water mass as a function of RH at $T = 298.15$ $[K]$. Fig. S6 shows the corresponding solid particulate matter (cases 11-20 in panels 1-10), panels 11-20 show the corresponding total dry particulate matter (PM), i.e., the sum of the liquid and solid aerosol mass (without aerosol water). Panels 1-10 of Fig. S7 show the total aerosol nitrate, while the panels 11-20 the aerosol ammonium concentration (both show cases 11-20).

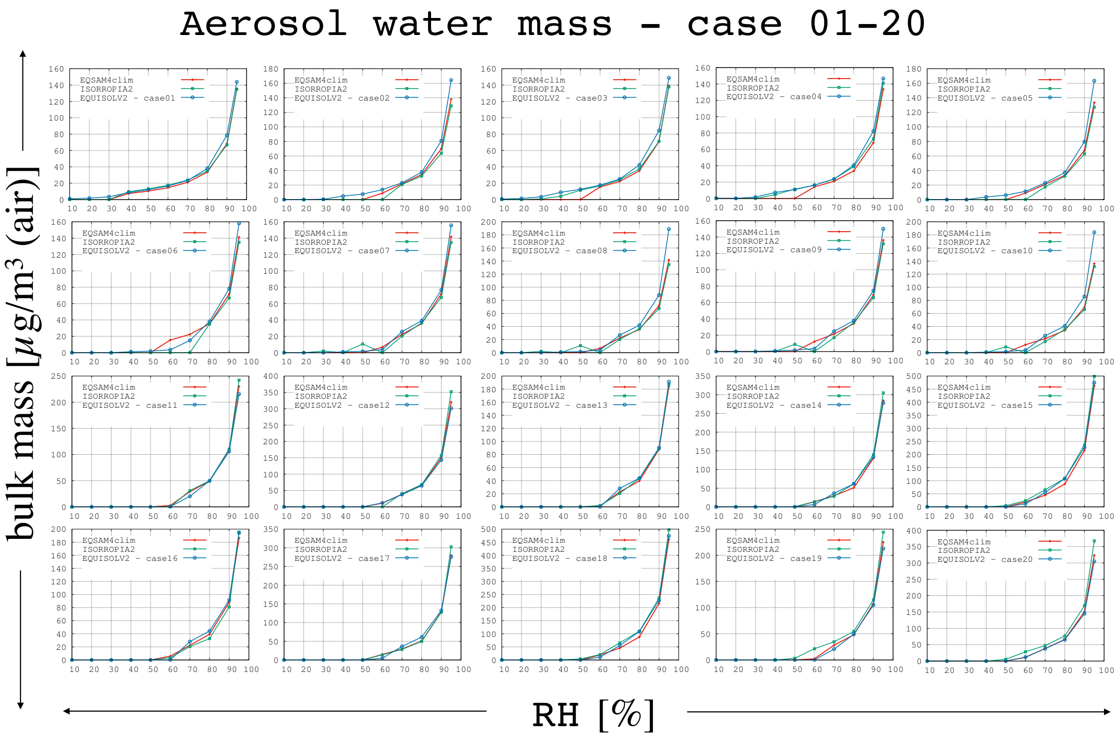

Figure S5: Extension of Figure 6 (main text): Bulk aerosol water mass as a function of RH for various sulfate molar ratios, fixed for the entire RH range (at constant $T = 298.15$ K). Only the dry concentration ratio varies from case to case to match the domains of Table 2. The 20 aerosol composition cases refer to Table 3 of Xu et al. (2009). A subset of four panels is shown in the following for better reading.

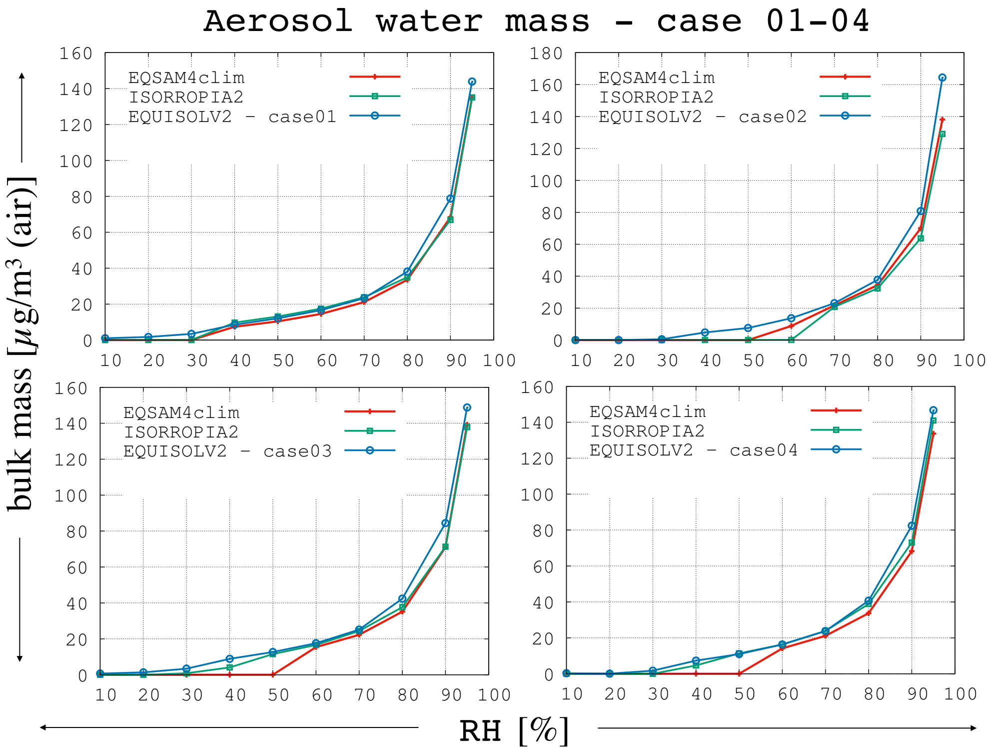

Figure S5.1: Case 1-4 of Figure S5 (Supplement).

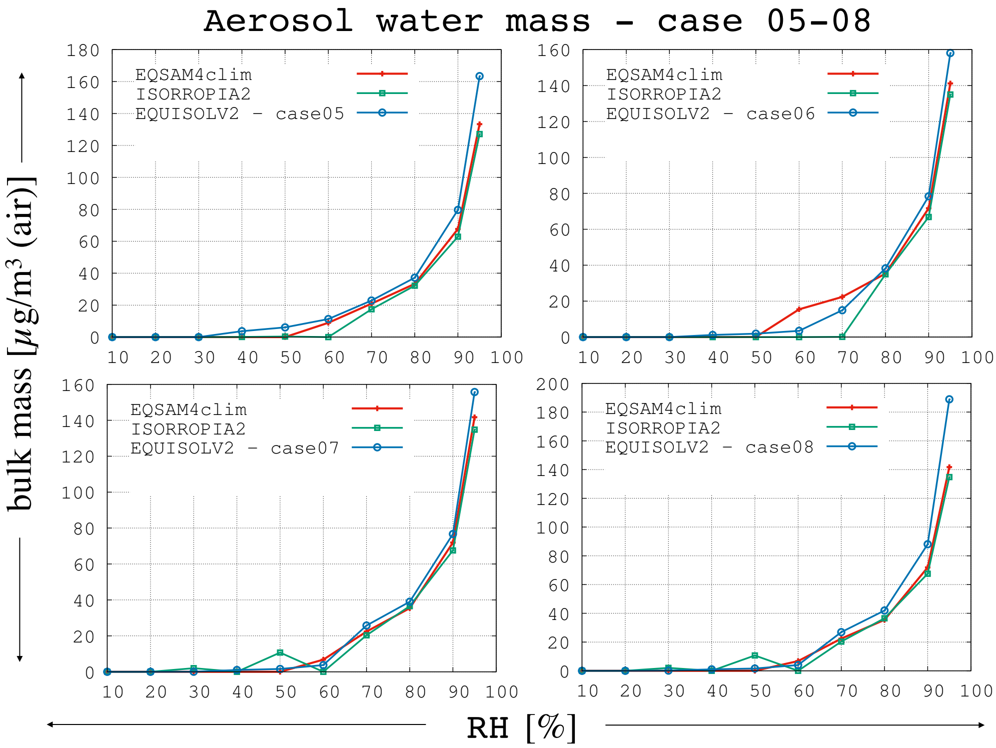

Figure S5.2: Case 5-8 of Figure S5 (Supplement).

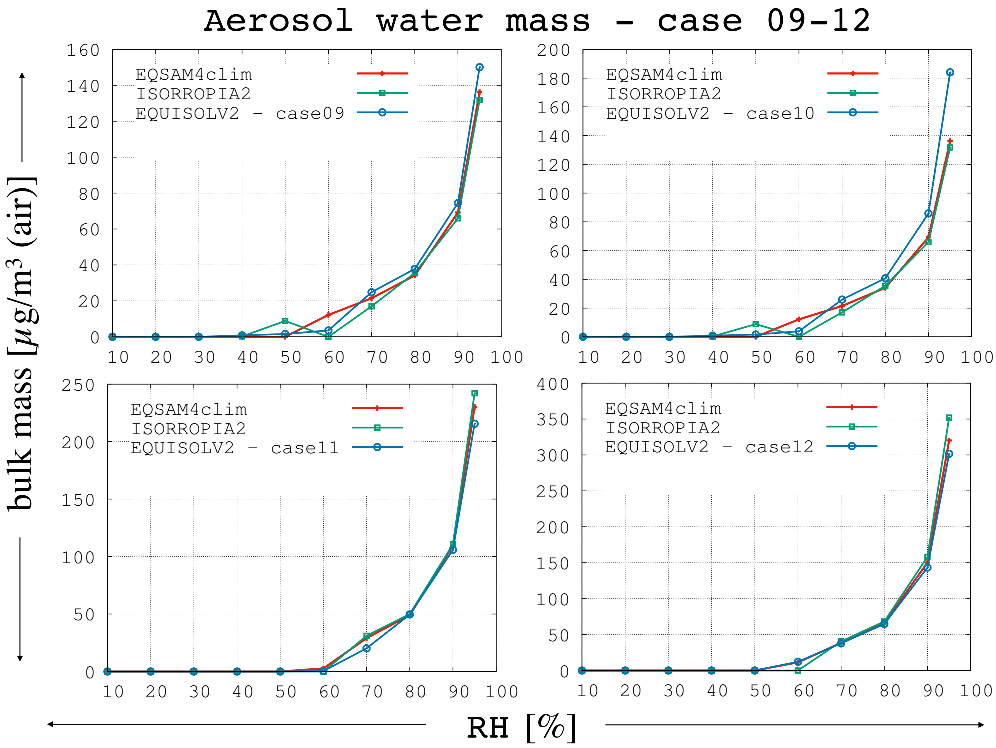

Figure S5.3: Case 9-12 of Figure S5 (Supplement).

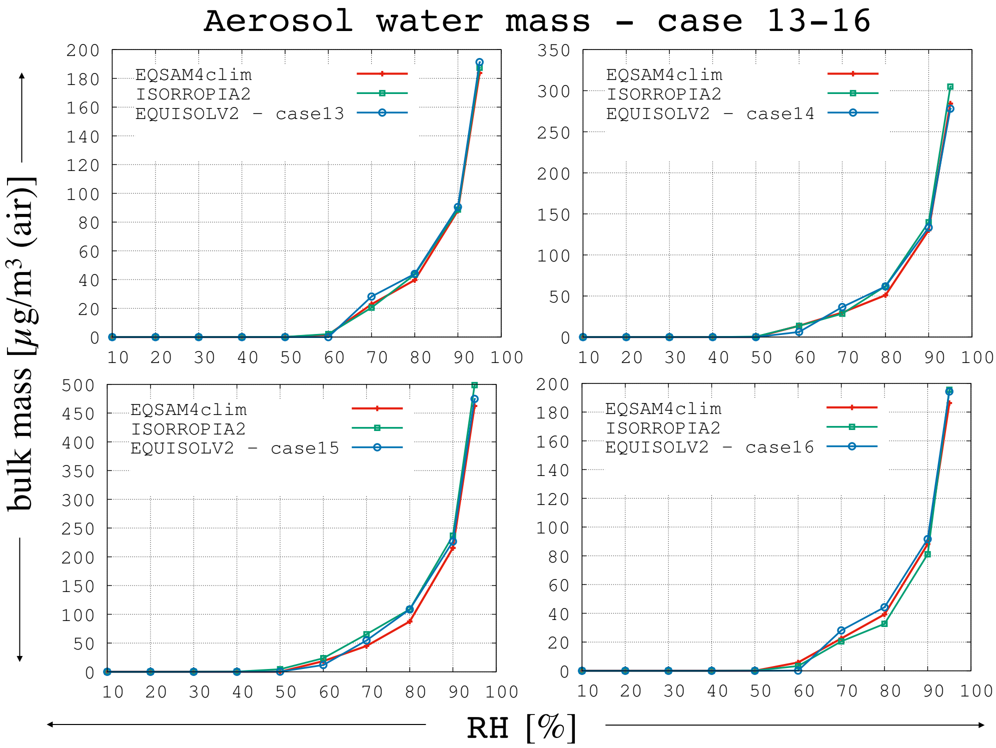

Figure S5.4: Case 13-16 of Figure S5 (Supplement).

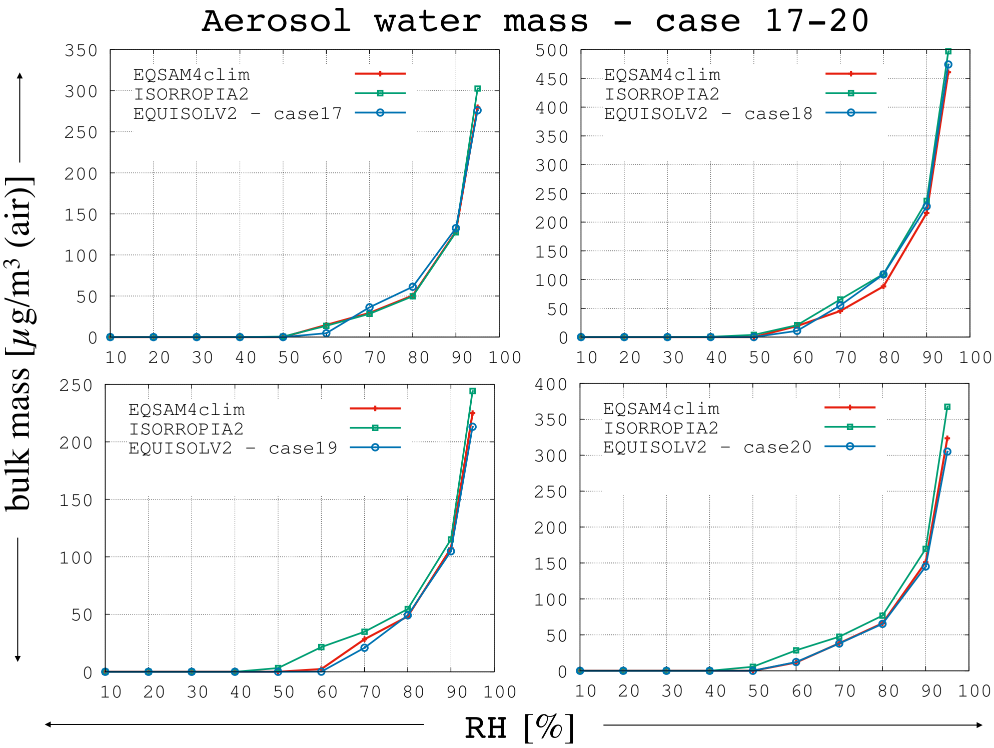

Figure S5.5: Case 17-20 of Figure S5 (Supplement).

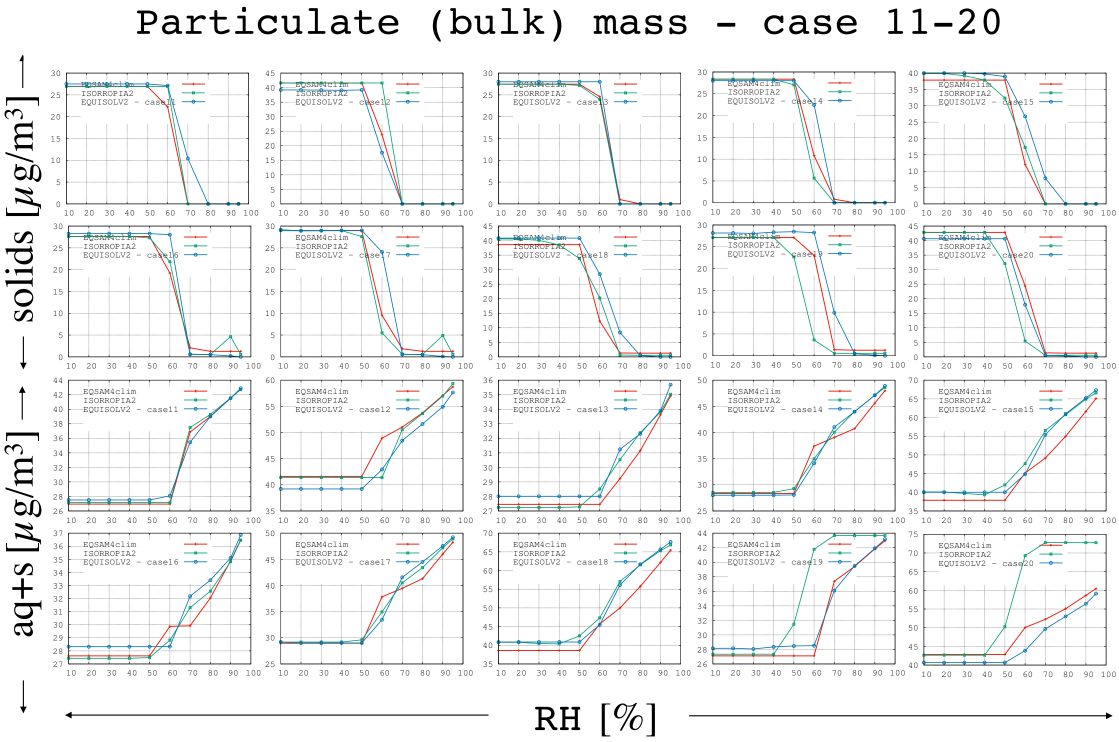

Figure S6: Extension of Figure 7 (main text): Total solid PM and liquid+solid PM.

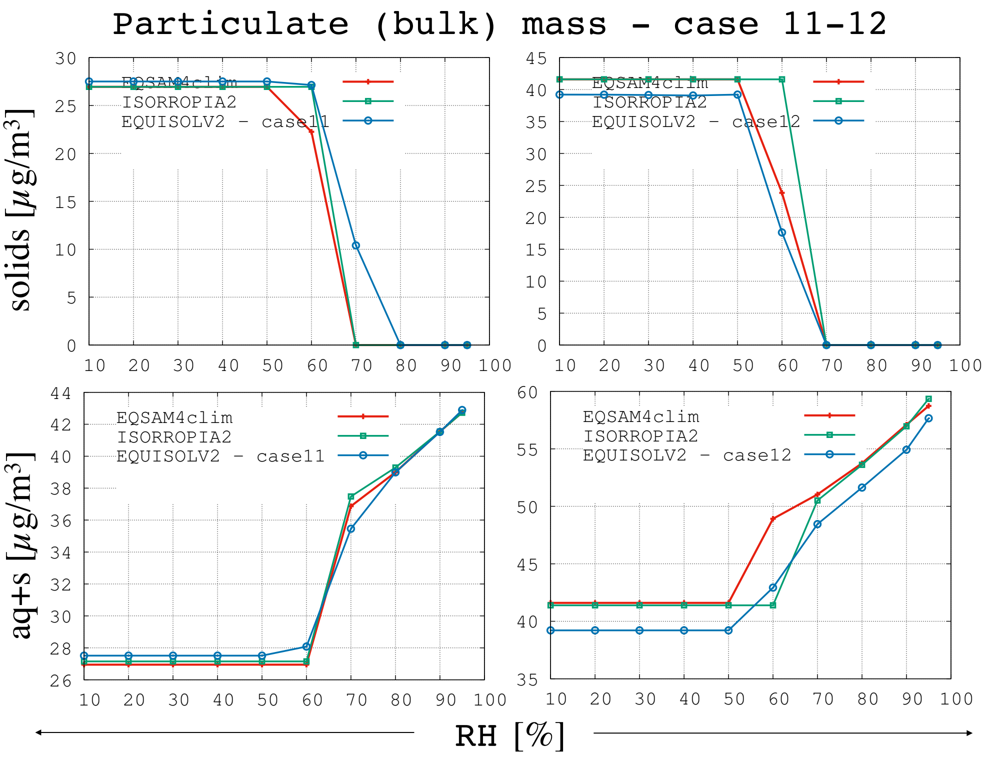

Figure S6.1: Case 11-12 of Figure S6 (Supplement).

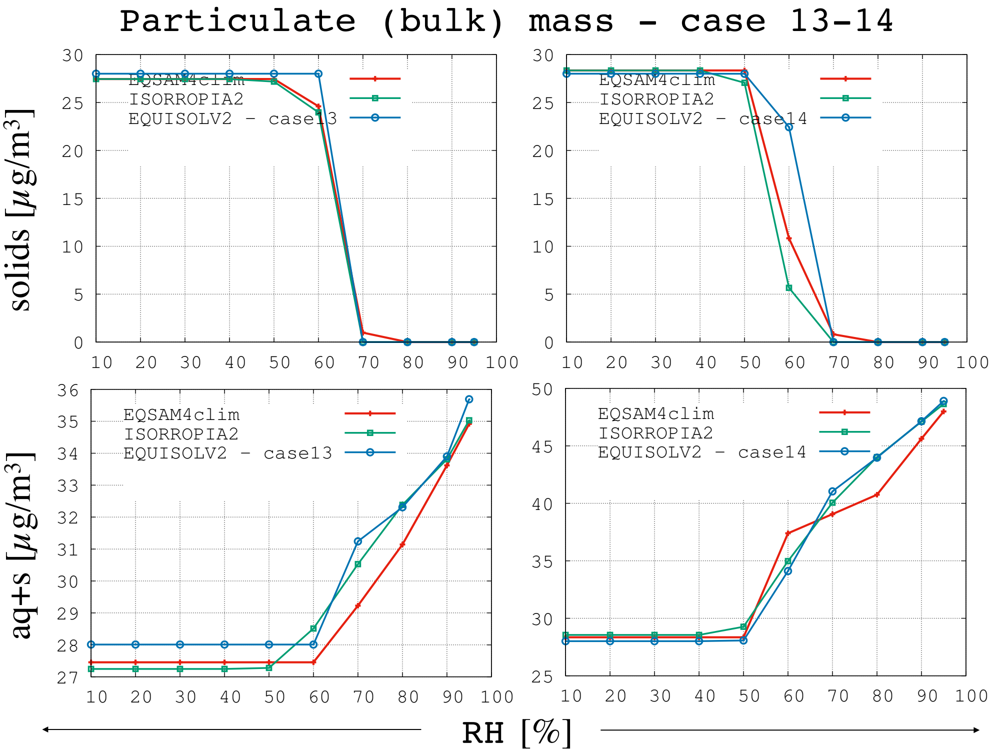

Figure S6.2: Case 13-14 of Figure S6 (Supplement).

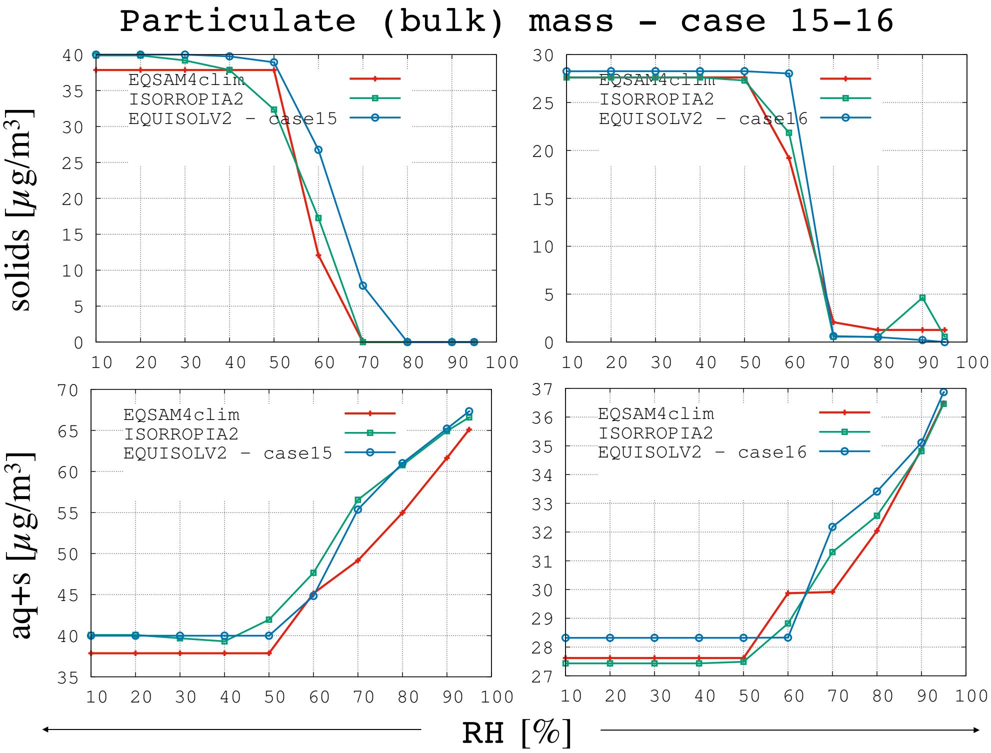

Figure S6.3: Case 15-16 of Figure S6 (Supplement).

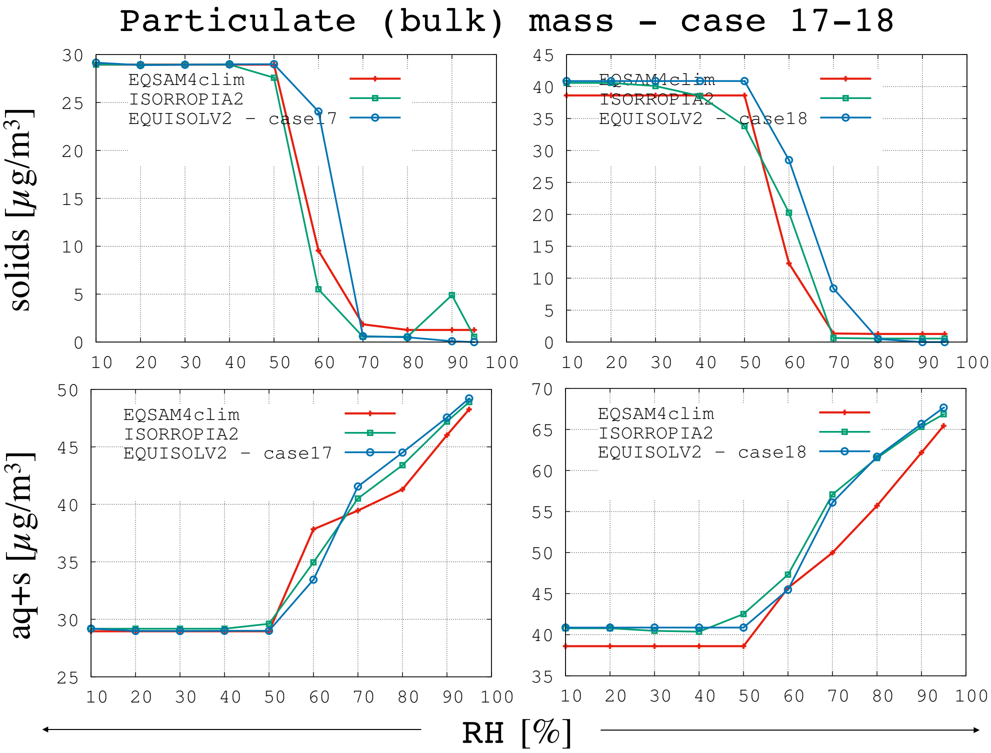

Figure S6.4: Case 17-18 of Figure S6 (Supplement).

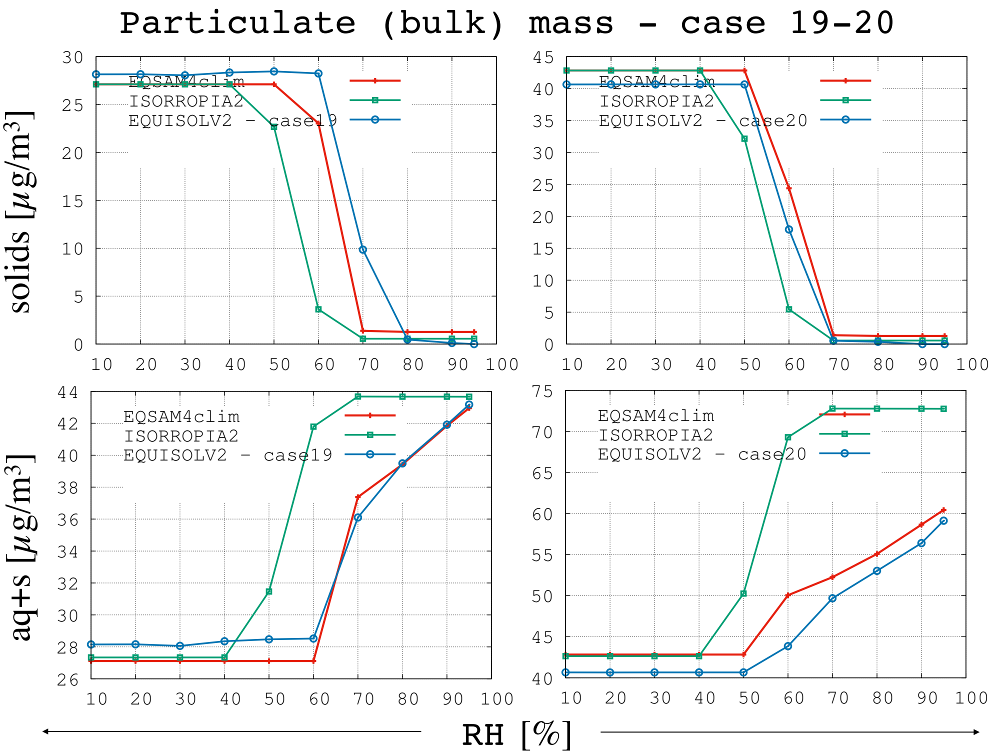

Figure S6.5: Case 19-20 of Figure S6 (Supplement).

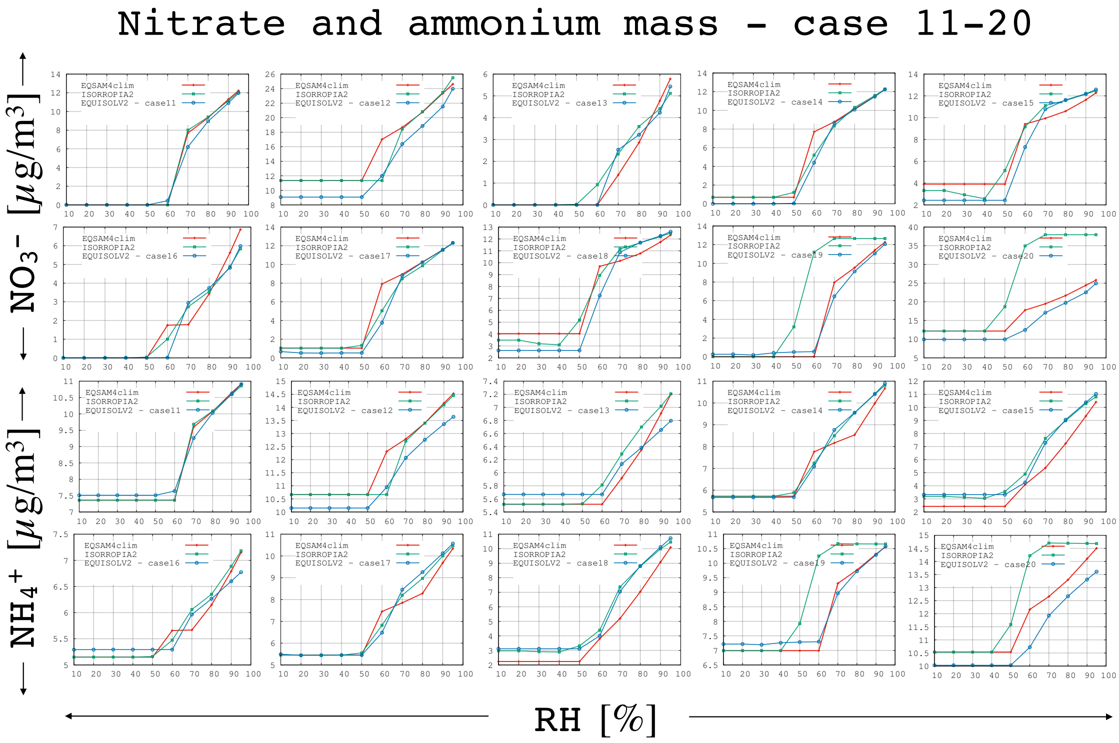

Figure S7: Extension of Figure 7 (main text): Bulk aerosol nitrate and ammonium.

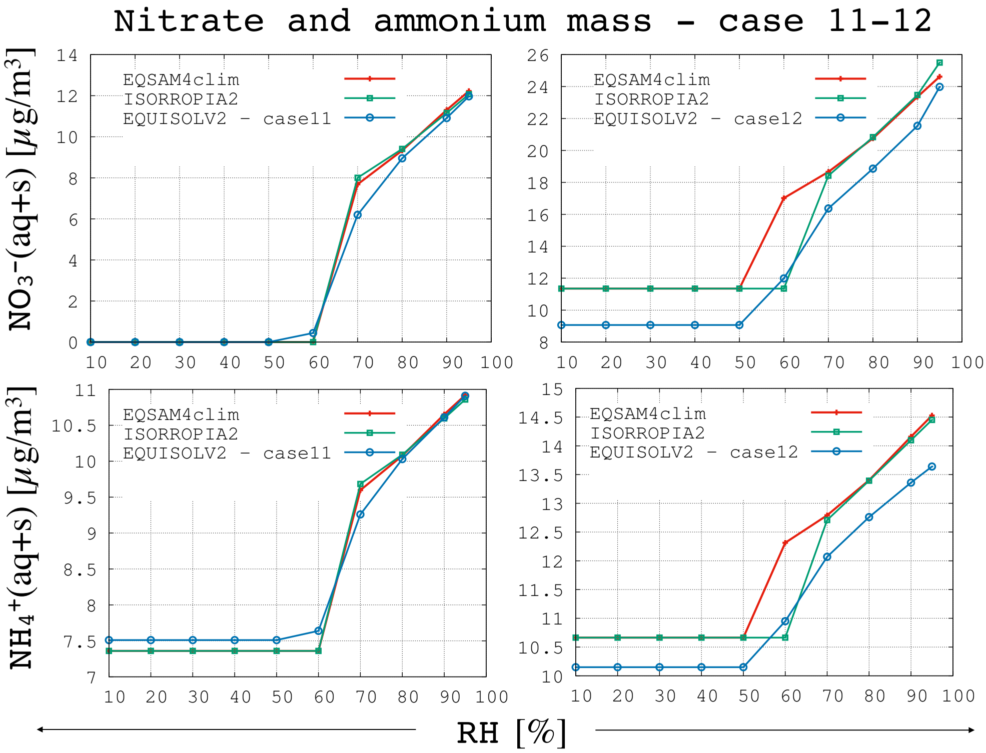

Figure S7.2: Case 11-12 of Figure S7 (Supplement).

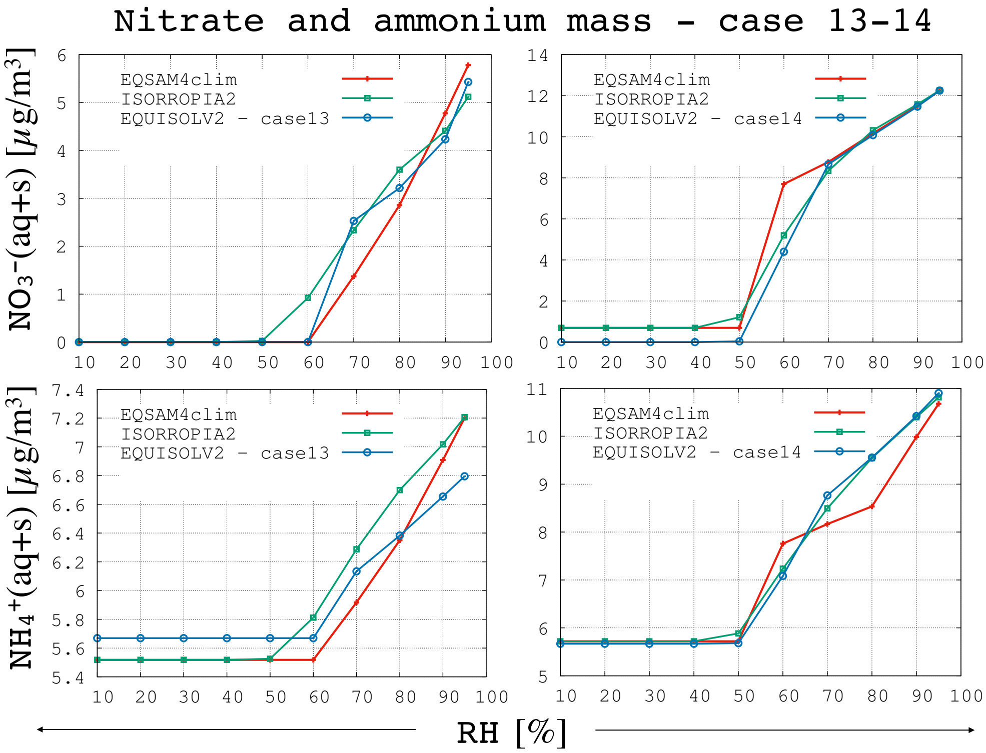

Figure S7.3: Case 13-14 of Figure S7 (Supplement).

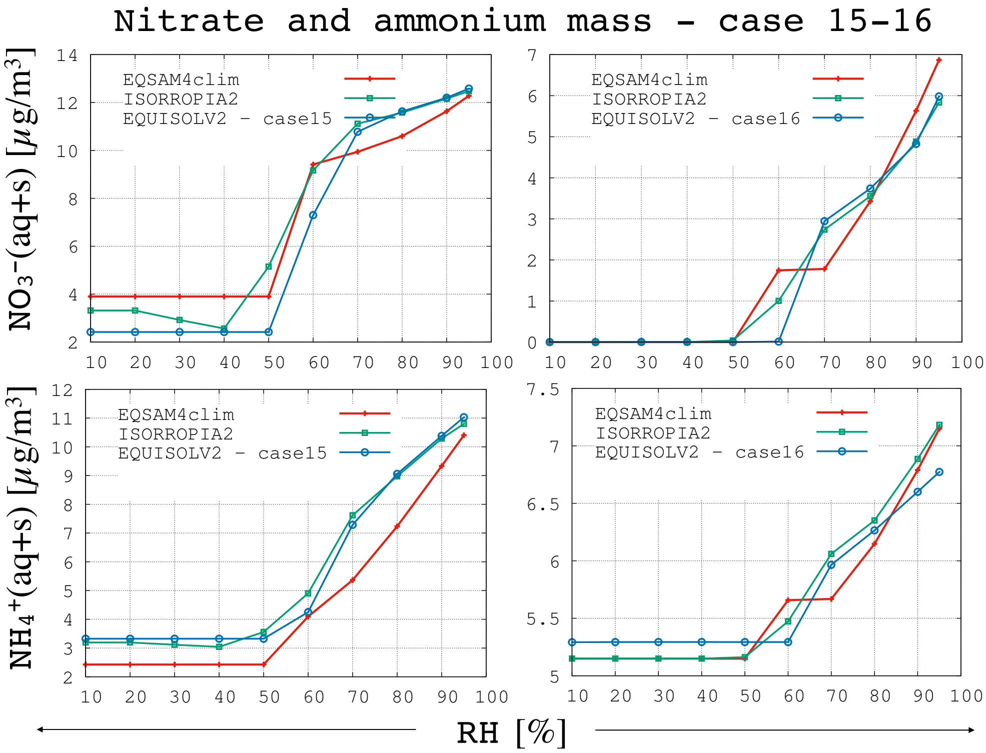

Figure S7.4: Case 15-16 of Figure S7 (Supplement).

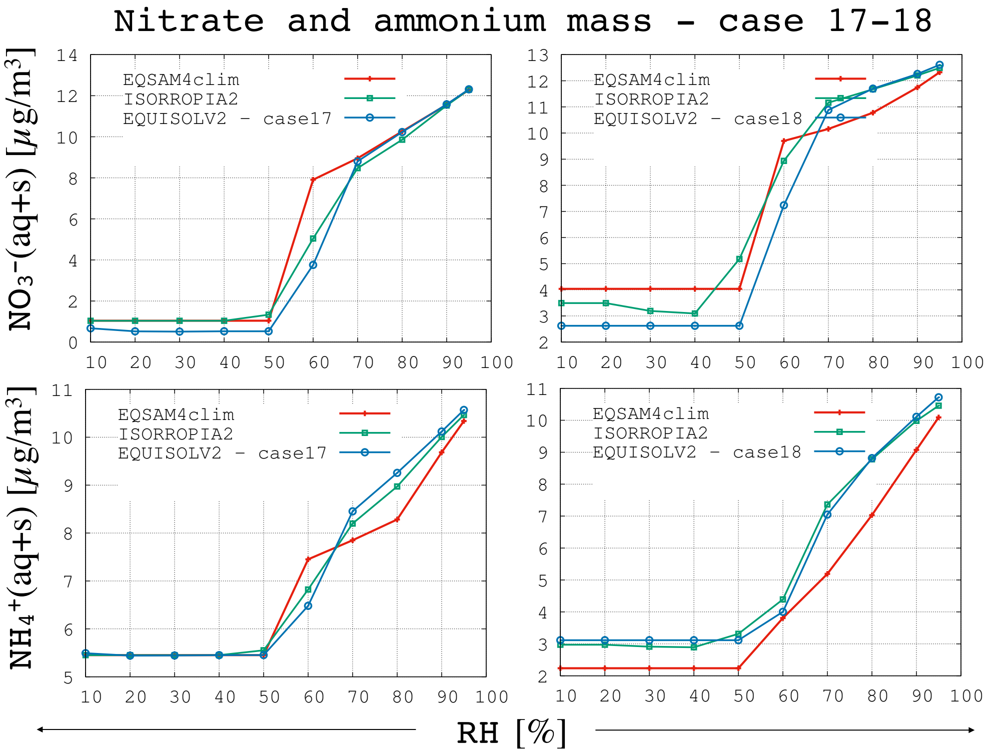

Figure S7.5: Case 17-18 of Figure S7 (Supplement).

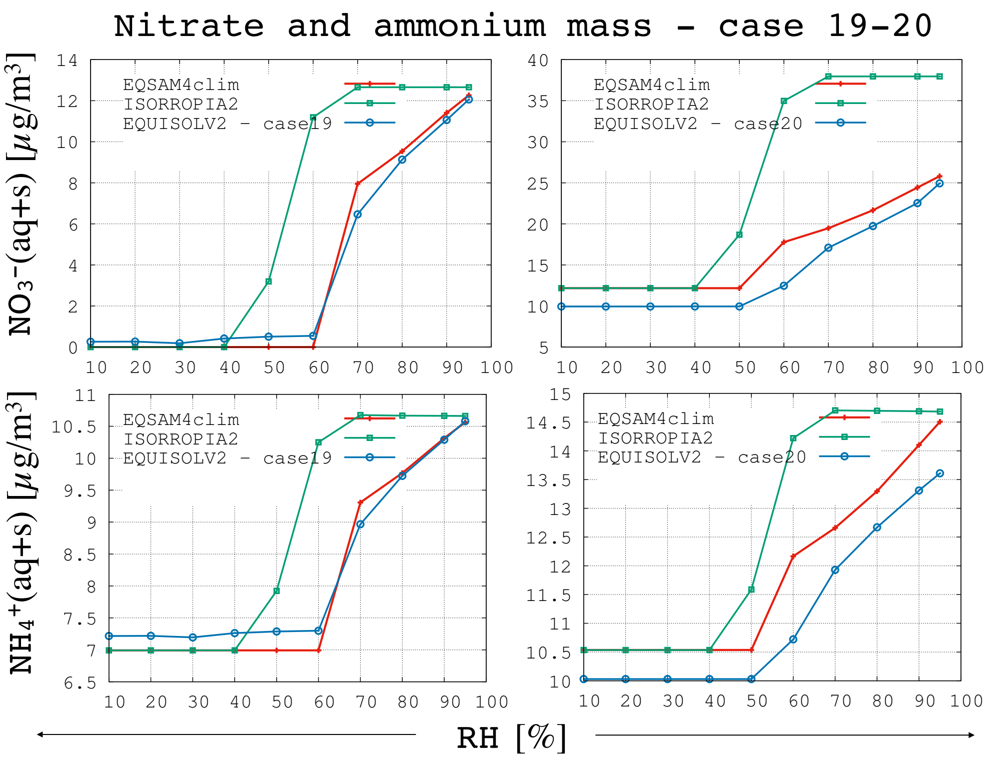

Figure S7.6: Case 19-20 of Figure S7 (Supplement).

S3.4 Field observations – MINOS campaign

Extension of Figure 8 and 9 of Sec. 3.4. Figures S8 and Figure S9 show the gas-liquid-solid partitioning results of EQSAM4clim (red crosses) and ISORROPIA II (green squares). The equilibrium computations are based on lumped cation and anion concentrations, which were observed during MINOS in the aerosol fine and coarse mode, respectively. Fig. S8, panels (1-20), show the model results for the aerosol fine mode (from left to right, top to bottom): total aerosol water mass $[\mu g/m^3(air)]$, total particulate (aqueous+solid) matter (PM) $[\mu g/m^3(air)]$, total solid PM $[\mu g/m^3(air)]$, total (aqueous+solid) PM $[\mu mol/m^3(air)]$, and in $[nmol/m^3(air)]$ the (lumped) ion concentrations of: ammonium (NH_4^+), sodium (Na^+), potassium (K^+), calcium (Ca^{2+}), magnesium (Mg^{2+}), sulfate (SO_4^{2-}) – both as totals (aqueous+solid) and solids -, as well as total bi-sulfate (HSO_4^-) and the residual gases, hydrochloric acid (HCl), nitric acid (HNO_3) and ammonia (NH_3).

Fig. S9, panels (1-20), show the model results for the aerosol coarse mode (from left to right, top to bottom): total aerosol water mass $[\mu g/m^3(air)]$, total particulate (aqueous+solid) matter (PM) $[\mu g/m^3(air)]$, total solid PM $[\mu g/m^3(air)]$, total (aqueous+solid) PM $[\mu mol/m^3(air)]$, and in $[nmol/m^3(air)]$ the (lumped) ion concentrations of: ammonium (NH_4^+), sodium (Na^+), potassium (K^+), calcium (Ca^{2+}), magnesium (Mg^{2+}), sulfate (SO_4^{2-}), bi-sulfate (HSO_4^-), nitrate (NO_3^-), chloride (Cl^-), – all both as totals (aqueous+solid) and solids, except ammonium and bi-sulfate, which are omitted because of their very low (negligible) concentrations. Figures S8 and S9 are enlarged below, by Fig. S8.1-S8.5 and Fig. S9.1-S9.5, respectively to show the details. Despite the different approaches in the mixed solution treatment of EQSAM4clim and ISORROPIA II, EQSAM4clim is relatively close to the results of ISORROPIA II, capturing many details of the solid precipitation of individual compounds for both, the fine and coarse mode.

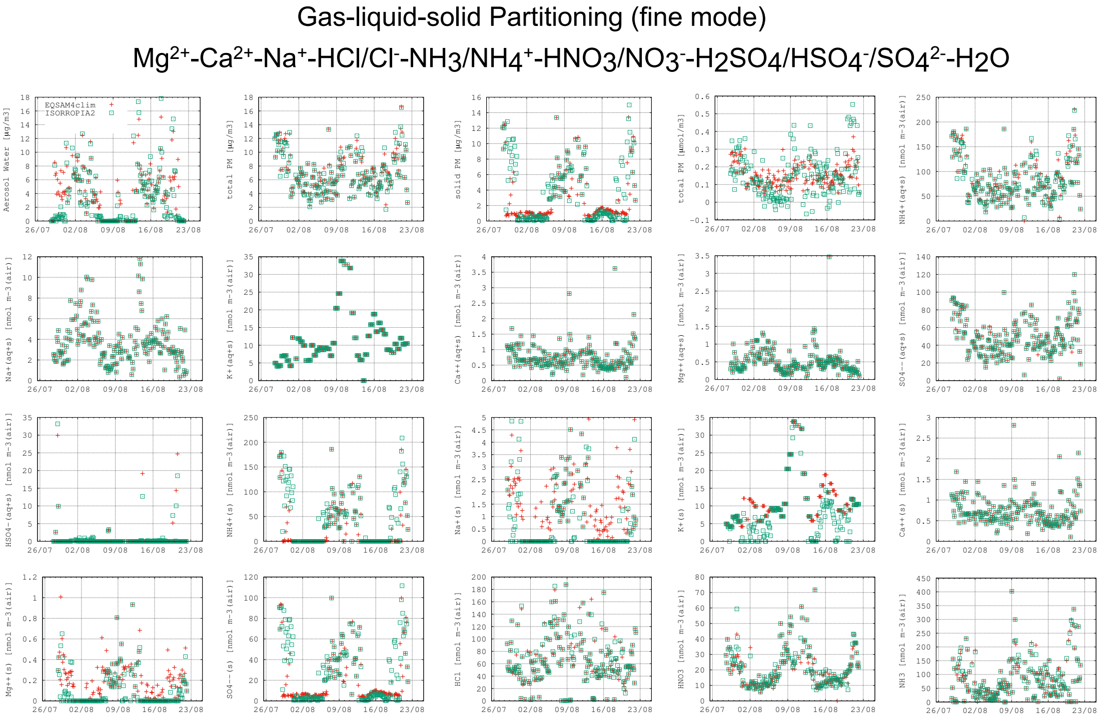
Gas-liquid-solid Partitioning (fine mode)

Mg^{2+}-Ca^{2+}-Na^{+}-HCl/Cl^{-}-NH_3/NH_4^{+}-HNO_3/NO_3^{-}-H_2SO_4/HSO_4^{-}/SO_4^{2-}-H_2O

Figure S8: Extension of Figure 8 (main text): Aerosol water, total particulate matter and total solids [$\mu g/m^3(air)$], the corresponding residual gases [$\mu mol/m^3(air)$], and various ions for the fine mode. EQSAM4clim (red crosses), ISORROPIA II (green squares). A subset of four panels is shown in the following for better reading.

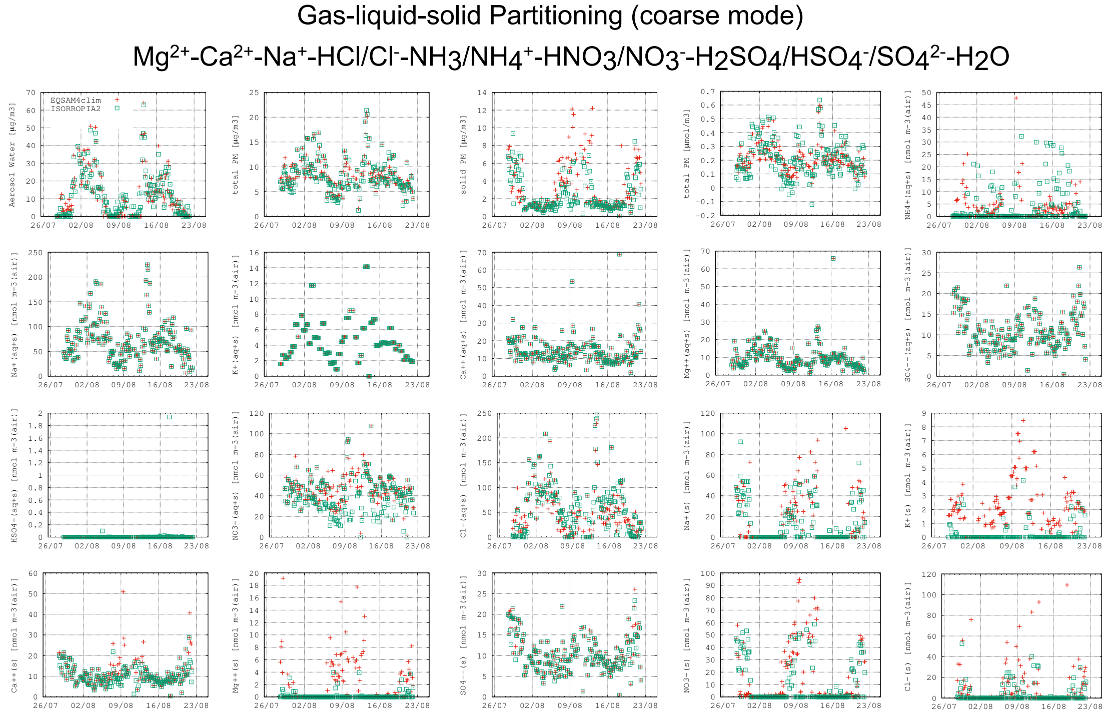
Gas-liquid-solid Partitioning (coarse mode)

Mg^{2+}-Ca^{2+}-Na^{+}-HCl/Cl^{-}-NH_3/NH_4^{+}-HNO_3/NO_3^{-}-H_2SO_4/HSO_4^{-}/SO_4^{2-}-H_2O

Figure S9: Extension of Figure S8 and Fig. 8 (main text) to the coarse mode.

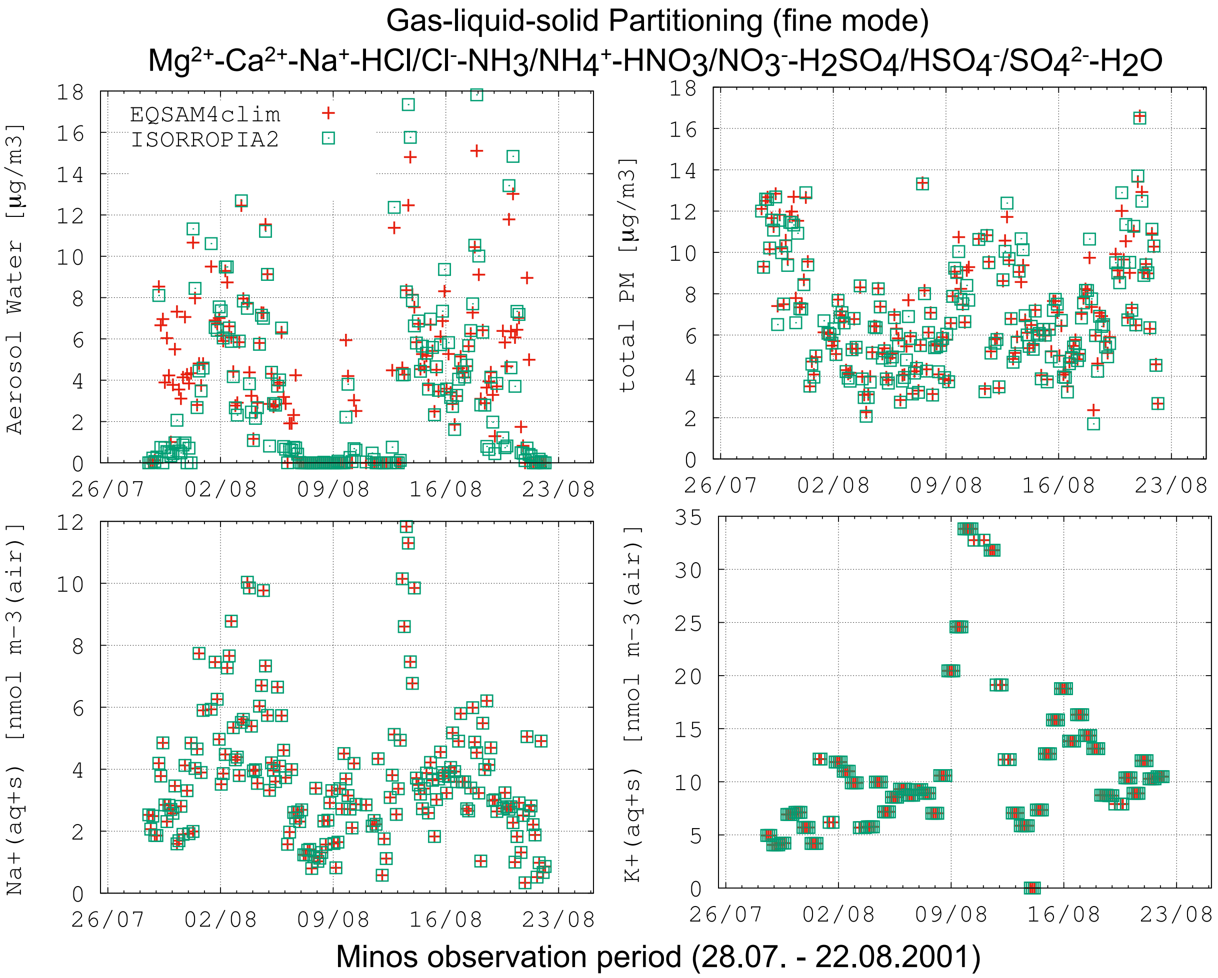

Figure S8.1: Details of Figure S8 (Supplement): Aerosol water(aq), total mass (aq+s), lumped Na^+(aq+s) and K^+(aq+s) (nano moles).

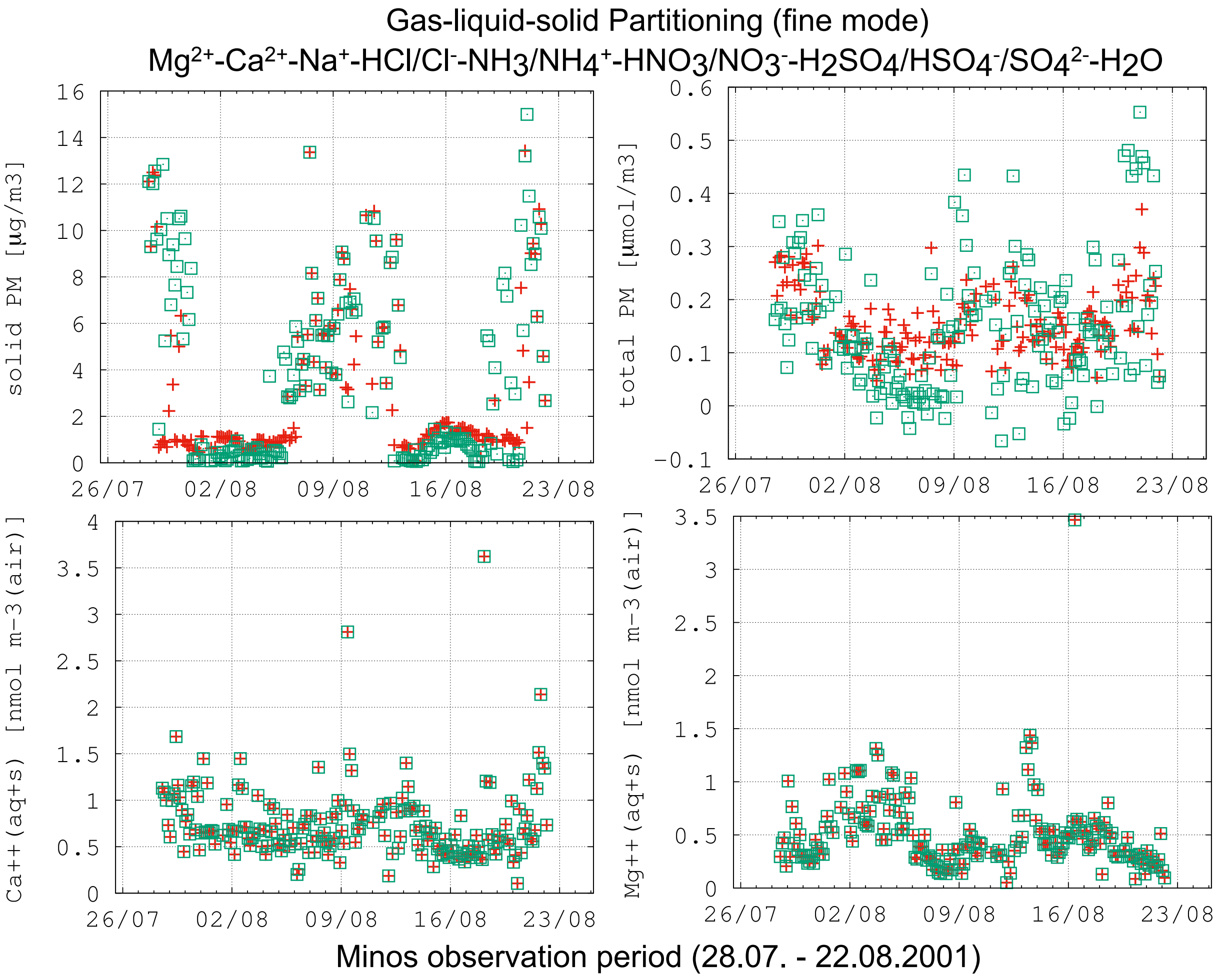

Figure S8.2: Details of Figure S8 (Supplement): solid mass(aq+s), total moles(aq+s), lumped Ca^{2+}(aq+s) and Mg^{2+}(aq+s) (nano moles).

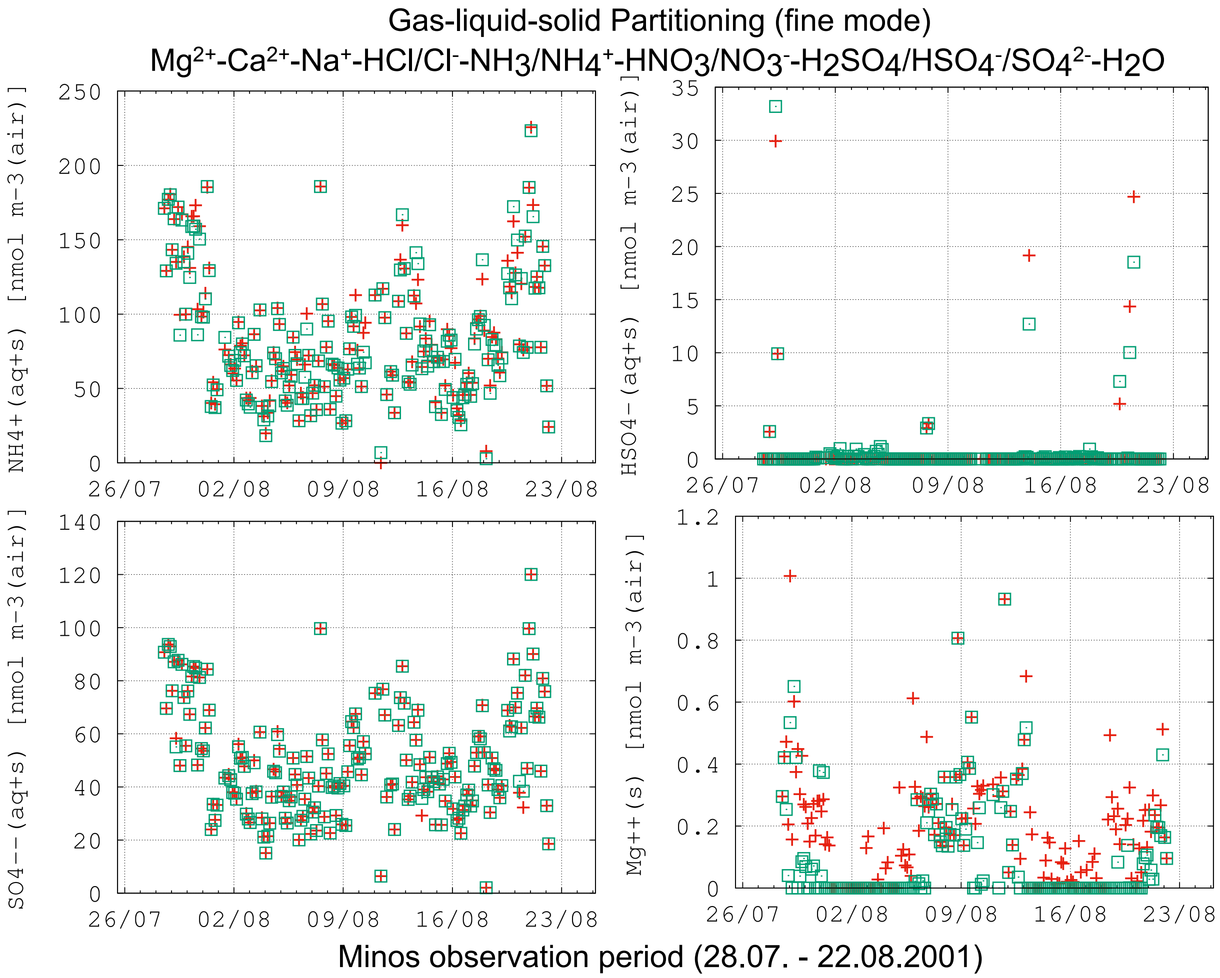

Figure S8.3: Details of Figure S8 (Supplement): Lumped NH_4^+(aq+s), HSO_4^-(aq+s), SO_4^{2-}(aq+s) and Mg^{2+}(s) (nano moles).

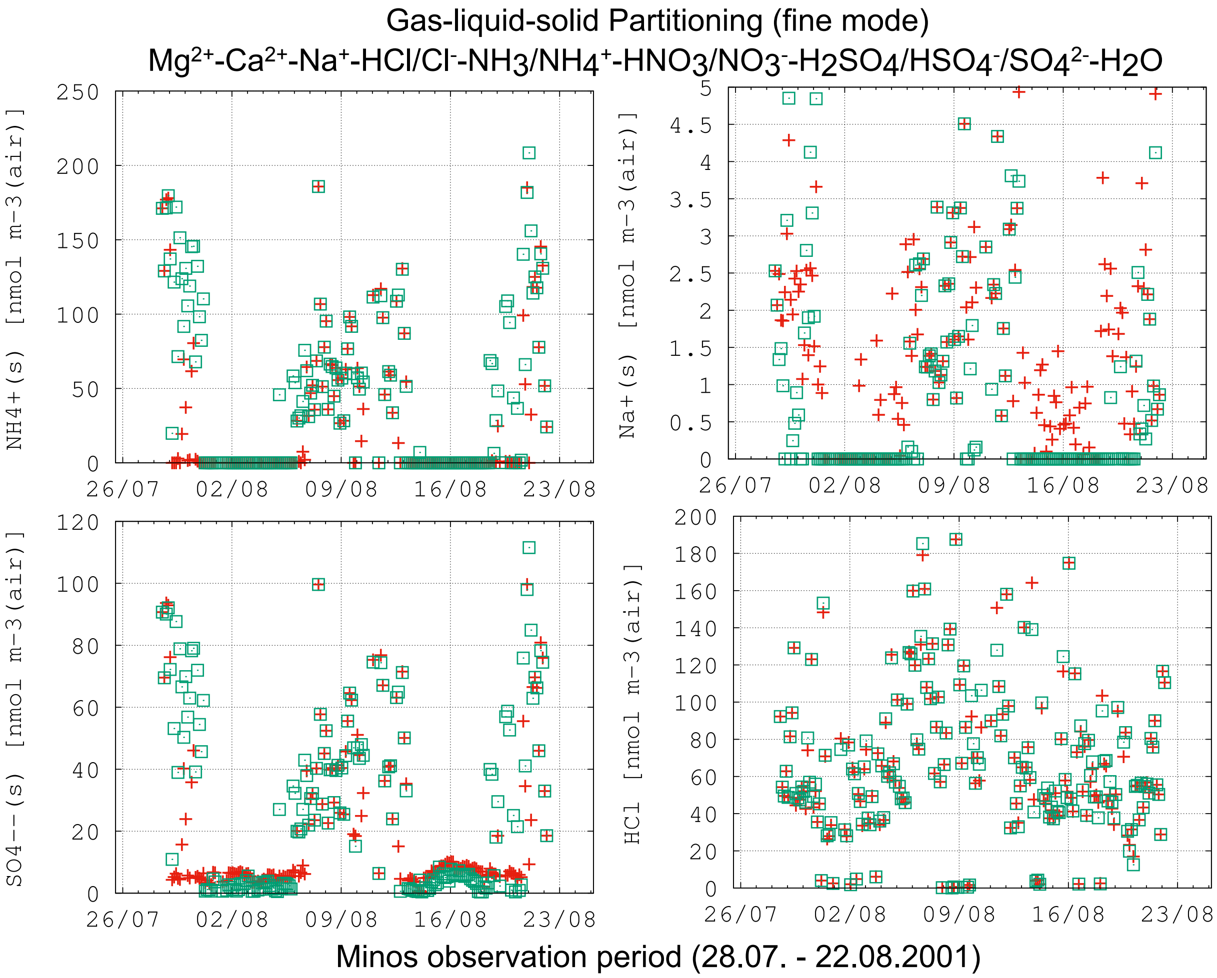

Figure S8.4: Details of Figure S8 (Supplement): Lumped NH_4^+(s), Na^+(s), SO_4^{2-}(s) and HCl(g) (nano moles).

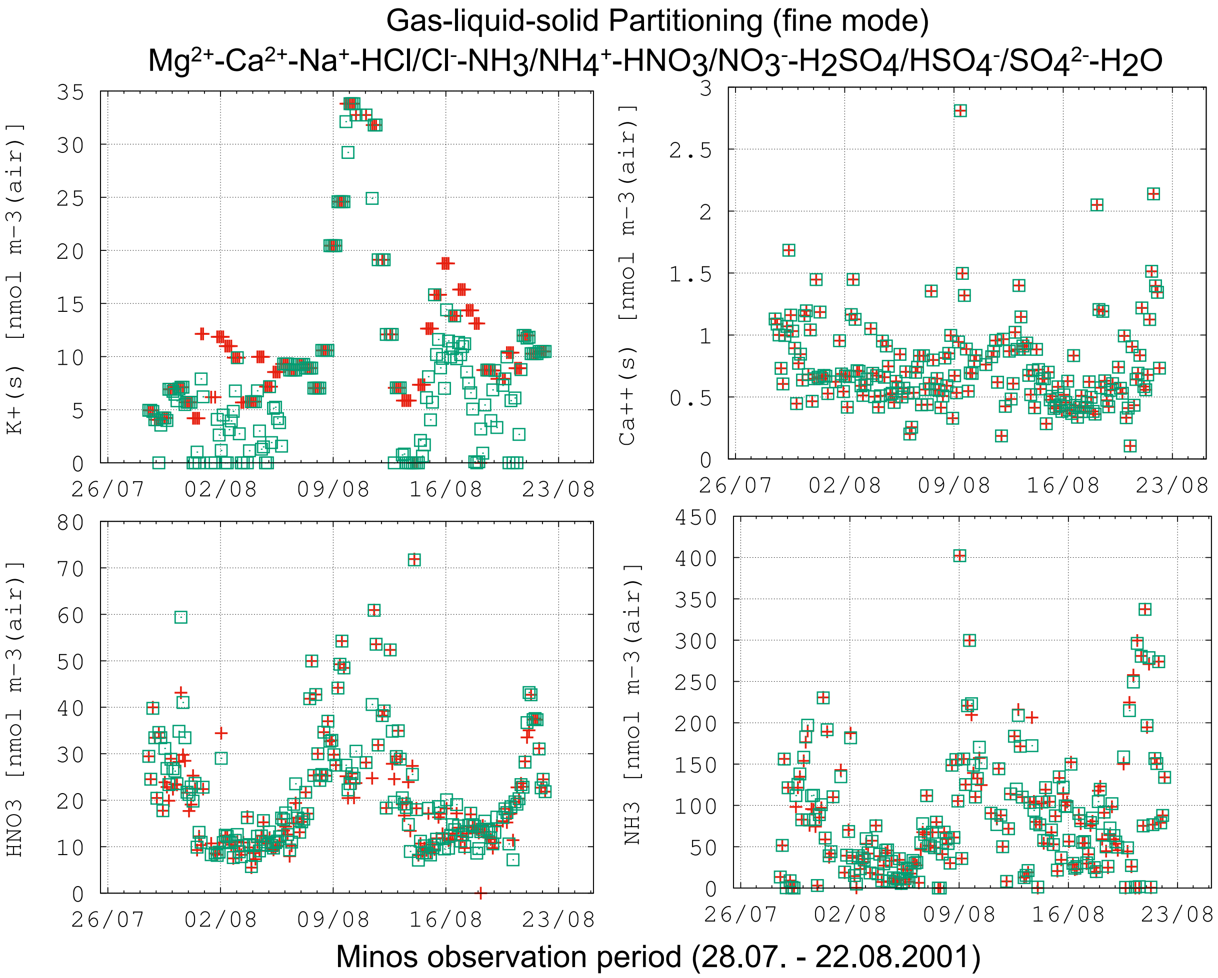

Figure S8.5: Details of Figure S8 (Supplement): Lumped $K^+(s)$, $Ca^{2+}(s)$, $HNO_3(g)$ and $NH_3(g)$ (nano moles).

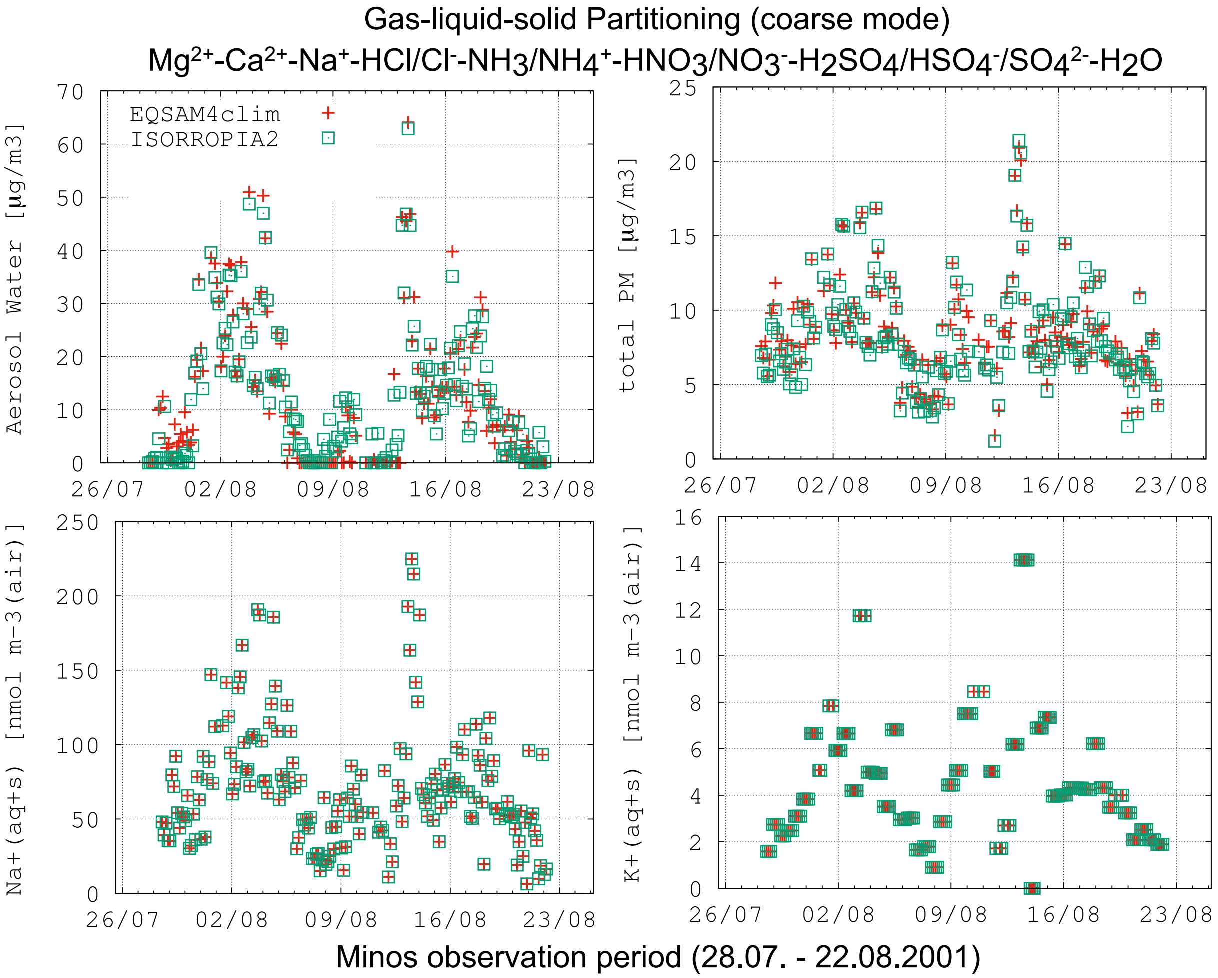

Figure S9.1: Details of Figure S9 (Supplement): Aerosol water(aq), total mass (aq+s), lumped Na^+(aq+s) and K^+(aq+s) (nano moles).

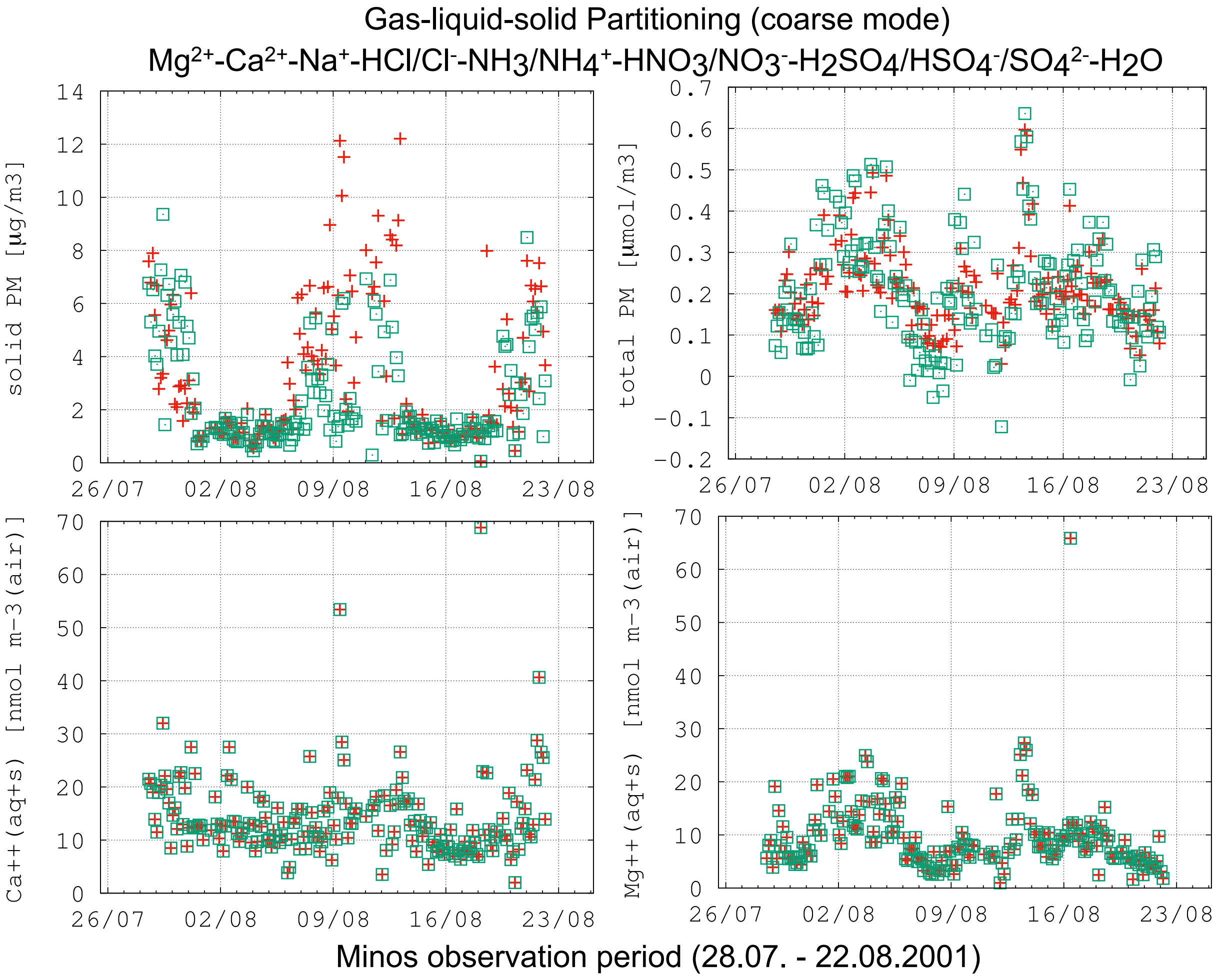

Figure S9.2: Details of Figure S9 (Supplement): solid mass(aq+s), total moles(aq+s), lumped Ca^{2+}(aq+s) and Mg^{2+}(aq+s) (nano moles).

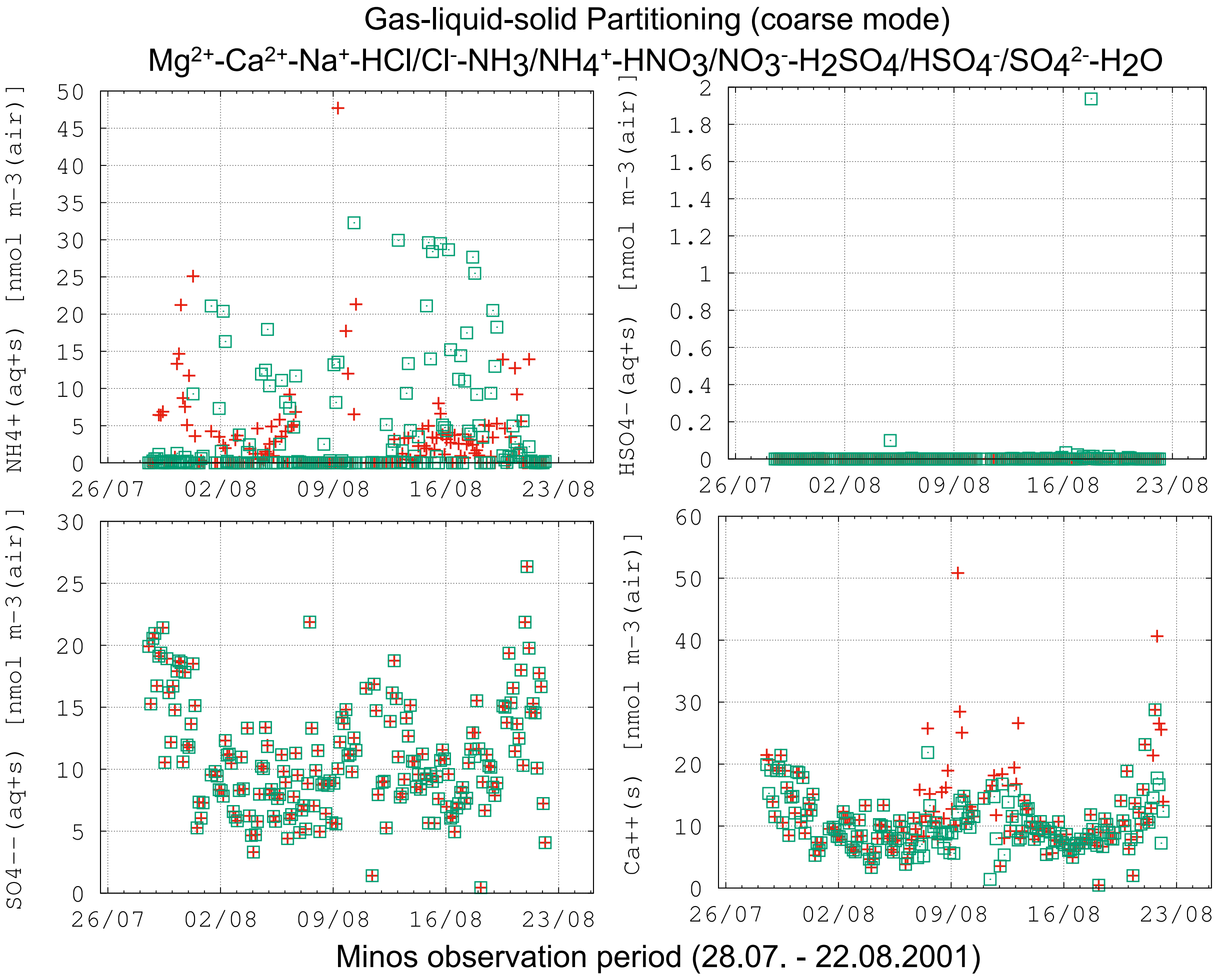

Figure S9.3: Details of Figure S9 (Supplement): Lumped $NH_4{}^+$(aq+s), $HSO_4{}^-$(aq+s), $SO_4{}^{2-}$(aq+s) and Ca^{2+}(s) (nano moles).

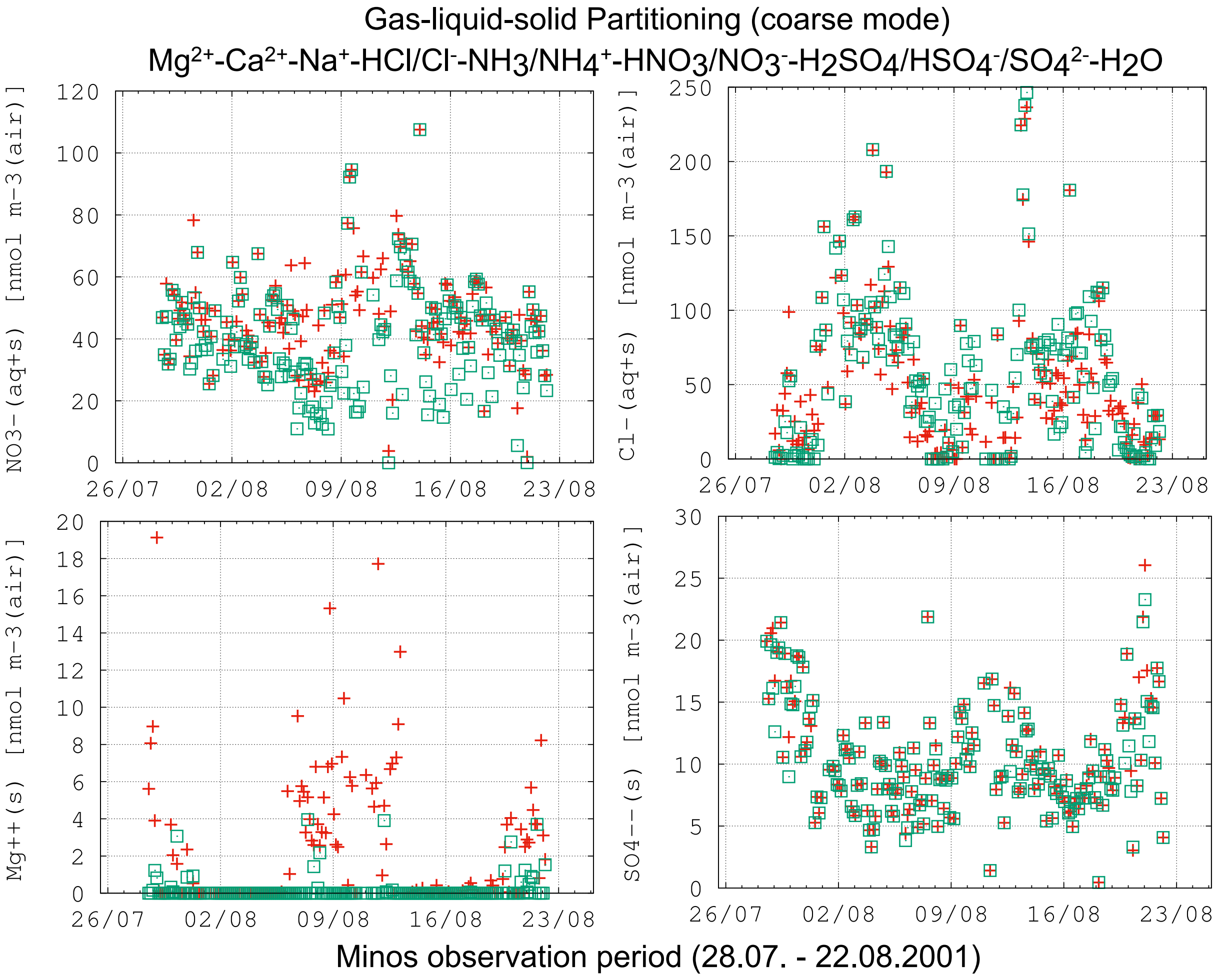

Figure S9.4: Details of Figure S9 (Supplement): Lumped $NO_3{}^-$(aq+s), Cl^-(aq+s), Mg^{2+}(s) and $SO_4{}^{2-}$(s) (nano moles).

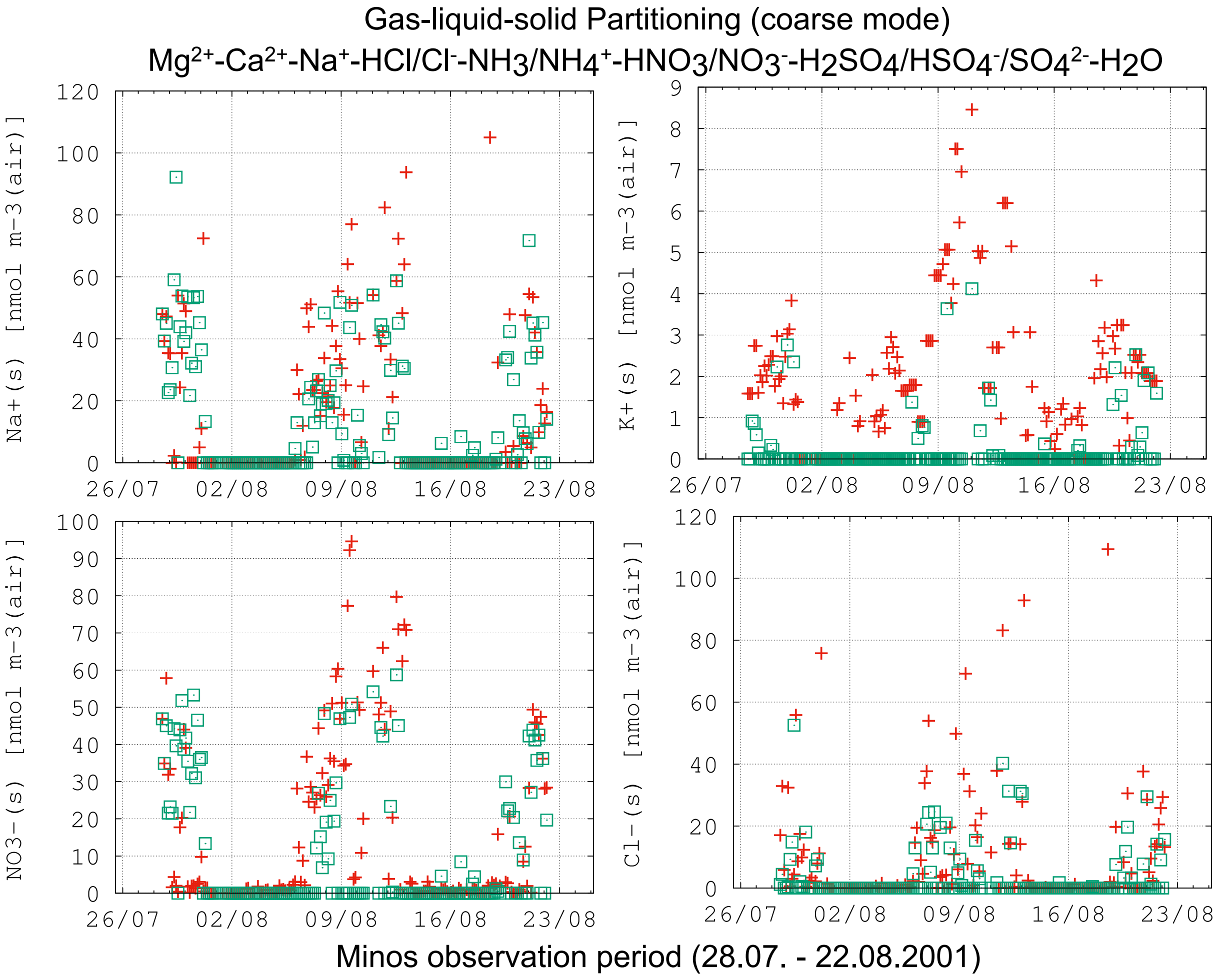

Figure S9.5: Details of Figure S9 (Supplement): Lumped Na^+(s), K^+(s), $NO_3{}^-$(s) and Cl^-(s) (nano moles).